AGRICULTURE

The microRNA OsmiR393 regulates rice brown planthopper resistance by modulating the auxin–ROS signaling cross-talk

Lin Zhu[1,2,3]†, Haichao Li[2]†, Zhihuan Tao[2,3], Feilong Ma[4], Shujun Wu[1], Xuexia Miao[2]*, Liming Cao[1]*, Zhenying Shi[1]*

Auxin plays critical roles in plant development and stress response. However, the roles of auxin and the immune signaling factor, reactive oxygen species (ROS), in resistance to the brown planthopper (BPH), a notorious rice-specific piercing–sucking insect that causes severe yield losses, remain unclear. We revealed that moderate naphthalene acetic acid treatment activates rice resistance to BPH, BPH infestation induces ROS accumulation, and increase in ROS content promotes BPH resistance. Underlying these phenomena, the auxin receptors OsTIR1 and OsAFB2 positively, whereas the posttranscriptional regulator OsmiR393 negatively, regulate BPH resistance. Downstream of the OsmiR393/OsTIR1 module, through successive genetic function analysis of each gene, solid genetic relationship analysis, and various biochemical assays, we established an OsmiR393/OsTIR1-OsIAA10-OsARF12-OsRbohB genetic pathway that mediates BPH resistance, in which ROS are integral. Such cross-talk between auxin and ROS reveals the intricate signaling network underlying BPH resistance, which might assist with BPH resistance breeding.

INTRODUCTION

Rice (*Oryza sativa* L.) is a staple food that sustains more than half of the global population. Brown planthopper (BPH; *Nilaparvata lugens* Stål) is the most notorious insect pest specific to rice. BPH causes direct harm to the host, through its long, piercing mouthparts, and also causes indirect harm by transmitting a variety of virus. In rice-growing areas, the annual yield loss caused by BPH is estimated to exceed US$300 million dollars (*1*), which is much higher than that caused by other pathogens in recent years. Compared with chemical-based and natural enemy–based approaches, the use of rice endogenous resistance has the advantages of providing effective, long-lasting, and environment-friendly protection. Therefore, extensive efforts have been made to identify BPH resistance genes in rice in recent decades. Till now, more than 40 of them have been identified, and 17 of them been successfully isolated by map-based cloning.

BPH resistance genes assist rice plants to activate downstream defense-related signaling pathways, which interconnected to enable the plants to rapidly execute to a cost-effective response. Phytohormones are essential regulators of plant development and immune signaling against biotic stresses such as pathogen and insect herbivores, as well as abiotic stresses (*2*). Auxin functions extensively in various processes in plant development and physiology. Auxin signaling begins with the perception of auxin by the co-receptors auxin transport inhibitor response 1/auxin signaling F-box 2 (TIR1/AFB), which leads to degradation of auxin/indole-3-acetic acid (Aux/IAA) proteins through an ubiquitination mechanism, and thus releases the cognate auxin response factors (ARFs) to mediate downstream auxin signal transduction. Under auxin deficiency, the ARF proteins are repressed by Aux/IAA proteins and the compressor TOPLESS (TPL) (*3*, *4*). ARFs are transcription factors that bind specifically to the TGTCTC-containing auxin-responsive elements (AuxREs) in the promoters of early auxin-responsive genes (*5*, *6*). Increasing evidence suggests that ARFs are crucial for plant response to various abiotic and biotic stresses (*7*). Successful microbial infection can disturb auxin signaling in the host plants to promote disease development, and, in turn, auxin may affect the pathogen to enhance its virulence (*8*). Auxin signaling increases the susceptibility of *Arabidopsis* plants to the root-infecting fungus *Fusarium oxysporum* (*9*). Rice dwarf virus (RDV) realizes infection through interaction of the P2 capsid protein with OsIAA10, thereby preventing OsIAA10 from degradation (*10*). OsARF17 interacts with proteins of different viruses and is functionally repressed to facilitate infection (*11*). However, the functions of OsARFs vary. For example, *OsARF12* and *OsARF16* positively, whereas *OsARF11* negatively, regulate resistance to RDV (*12*). However, the role of auxin signaling in rice-BPH interaction remains unknown.

Production of reactive oxygen species (ROS) is a defense responses activated in plants upon different stresses (*13*, *14*). As a typical feature in pattern-triggered immunity (PTI), ROS mediate rapid, long-distance, cell-to-cell propagating signals in plants upon activation of plant immunity (*15*–*17*). ROS homeostasis is fine-tuned to avoid damage to the plant cells (*18*). The respiratory burst oxidase homologs (Rbohs) oxidize cytosolic reduced form of nicotinamide adenine dinucleotide phosphate and transfer the electrons to O_2, thereby generating superoxide, which is subsequently converted to hydrogen peroxide H_2O_2 (*19*). Hydrogen peroxide is recently identified as the primary mobile signal for sulfenylation of CCA1 HIKING EXPEDITION and increase in salicylic acid production in establishing systemic acquired resistance in *Arabidopsis* (*20*). Rbohs participate in defense against pathogen attacks by activating the hypersensitive responses and regulating innate immunity (*21*, *22*)

[1]Key Laboratory of Germplasm Innovation and Genetic Improvement of Grain and Oil Crops (Co-construction by Ministry and Province), Ministry of Agriculture and Rural Affairs, Crop Breeding and Cultivation Research Institute, Shanghai Academy of Agricultural Sciences, Shanghai 201403, China. [2]Key Laboratory of Plant Design, CAS Center for Excellence in Molecular Plant Sciences, Institute of Plant Physiology and Ecology, Chinese Academy of Sciences, Shanghai 200032, China. [3]University of Chinese Academy of Sciences, Beijing 100049, China. [4]Key Laboratory of Plant Genetics and Molecular Breeding, Zhoukou Normal University, Zhoukou 466001, China.
*Corresponding author. Email: zyshi@cemps.ac.cn (Z.S.); clm079@163.com (L.C.); xxm@cemps.ac.cn (X.M.)
†These authors contributed equally to this work.

and extracellular lignin production (*23*). However, direct evidence for the involvement of ROS signaling participating in BPH resistance remains elusive.

Plants rely on cross-talk between different signaling pathways to fine-tune the immune response. Downstream signaling events associated with ROS sensing involve Ca^{2+} and Ca^{2+}-binding proteins (*24*, *25*), activation of RHO-like small G proteins (*26*), mitogen-activated protein kinase (MAPK) (*27*), etc. Increased ROS production under stress influences the auxin and cytokinin networks, which function in the formation and maintenance of meristems (*28*). ROS functions as a downstream component in auxin-mediated signal transduction in root gravitropism (*29*). Auxin activates *Rboh* genes, enhances ROS production, and facilitates lateral root (LR) formation (*30*). Similarly, ROS signals mediate auxin-induced adventitious root formation in cucumber under waterlogging stress (*31*). Whether auxin and ROS cross-talk to mediate BPH resistance is unknown.

MicroRNAs (miRNAs) are increasingly being recognized as pivotal regulators in plant-environment interactions (*32*). Several miRNAs have been proved function in rice-BPH interaction. OsmiR396 negatively regulates BPH resistance by enhancing the flavonoid content mediated by *flavanone 3-hydroxylase* (*OsF3H*), a gene that positively regulates flavonoid biosynthesis and BPH resistance (*33*). Silencing of OsmiR156 enhances BPH resistance through reduction of jasmonic acid (JA) synthesis (*34*). OsmiR159 mediates BPH resistance through repression of the G protein γ subunit GS3 by the GAMYBL2 target and its influence on cellulose synthesis (*35*). OsmiR319 regulates BPH resistance through strong association between the target protein OsPCF5 and several OsMYB proteins that positively regulate BPH resistance (*36*). Quite a few typical factors in the auxin signaling pathway are posttranscriptionally regulated by miRNAs. For example, OsTIR1 and OsAFB2 are two targets of OsmiR393 (*37*). ARFs are respectively regulated by miR167-, miR160-, and miR390-phased TAS3 trans-acting small interfering RNAs influencing ARFs (https://www.mirbase.org/). Elucidation of the function of these auxin-mediating miRNAs in BPH resistance will enrich our knowledge of the role of auxin in rice-BPH interaction. Given that the targets of OsmiR393 are auxin receptors, we hypothesized that OsmiR393 may play a role in BPH resistance.

RESULTS

Auxin signaling activates rice resistance to BPH

To evaluate the role of auxin in rice resistance to BPH, we treated rice seedling plants with Naphthalene acetic acid (NAA), the analog of auxin, before feeding to BPH. Seven to 10 days later, when all the non-NAA–treated plants (non-treated) had died, the plants treated with 0.1 μM NAA remained alive, whereas most of the plants treated with 1 μM NAA died either (Fig. 1A). Accordingly, the survival rate of the 0.1 μM NAA-treated plants was much higher than that of non-treated plants, while that of the 1 μM-treated plants was intermediate (Fig. 1B), indicating that a low concentration of NAA activated BPH resistance, but, when the NAA concentration was raised, the promotive effect declined. In a parallel assay, the plants treated with 50 and 100 μM NAA died earlier than those non-treated plants

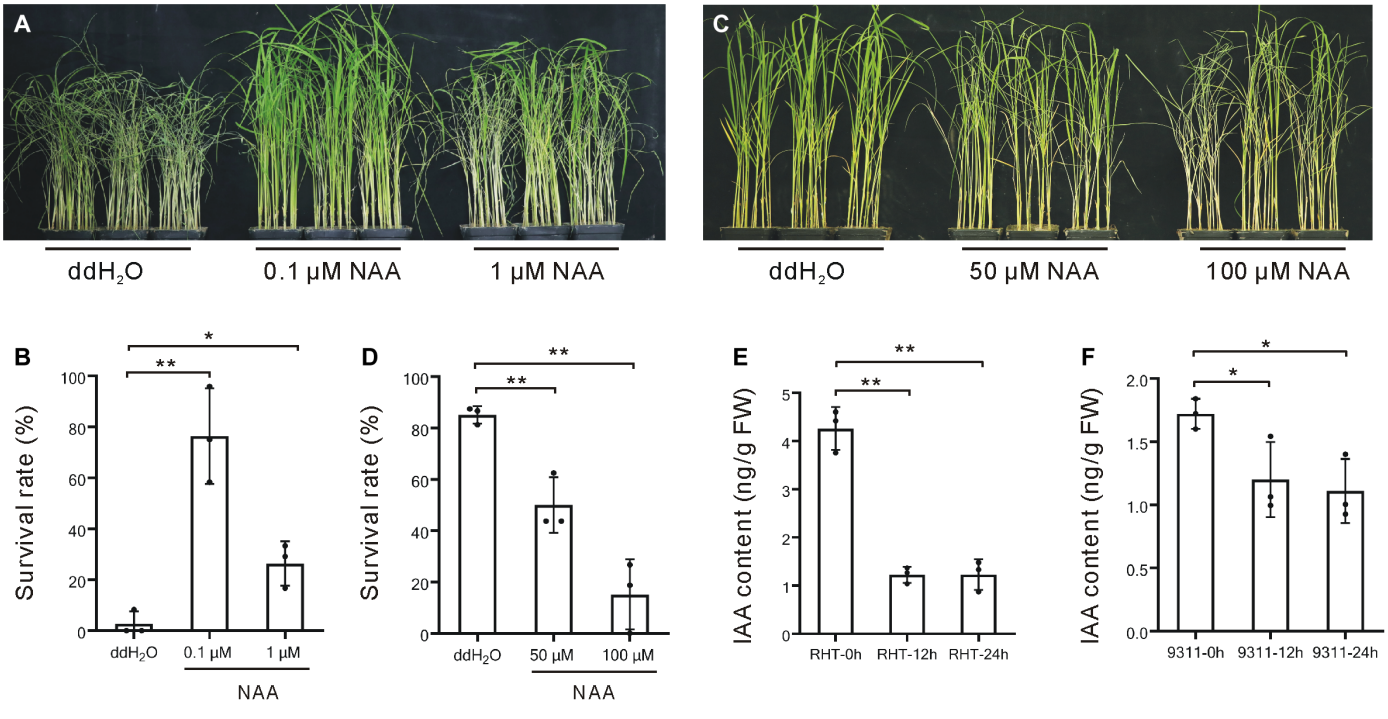

Fig. 1. Relationship between auxin and BPH infestation in rice. (**A**) BPH resistance of the rice plants treated with a low concentration (ddH$_2$O, 0.1 μM, and 1 μM) of NAA (ZH11 plants were used). (**B**) Survival rates of the plants in (A). Data are means ± SD ($n = 3$). (**C**) BPH resistance of the rice plants treated with a high concentration (ddH$_2$O, 50 μM, and 100 μM) of NAA. (**D**) Survival rates of the plants in (C). Data are means ± SD ($n = 3$). (**E**) IAA content before and after BPH infestation in the BPH-resistant rice cultivar RHT. Data are means ± SD ($n = 3$). (**F**) IAA content before and after BPH infestation in the BPH-susceptible rice cultivar 9311. Data are means ± SD ($n = 3$). Student's *t* test was carried out in [(B) and (D)] to compare with ddH$_2$O, in (E) to compare with RHT-0h, and in (F) to compare with 9311-0h (*$P < 0.05$; **$P < 0.01$). h, hours; FW, fresh weight.

(Fig. 1C), with a lower survival rate accordingly (Fig. 1D), confirming that treatment with a higher concentration of NAA treatment repressed the BPH resistance of rice plants.

Meanwhile, using the BPH-resistant rice cultivar "Rathu Heenati" (RHT) and the BPH-susceptible cultivar "9311" plants, we measured the endogenous IAA content after BPH infestation. In both cultivars, the IAA content decreased at 12 and 24 hours after BPH infestation, and the decrease in RHT was greater than that observed in 9311 (Fig. 1, E and F). Thus, BPH infestation lowered down the IAA content in the host plants.

Expression of the two main rice auxin receptors encoding genes, *OsTIR1* and *OsAFB2*, was induced in response to BPH infestation (fig. S1, A and B). Therefore, we constructed *OsTIR1*- and *OsAFB2*-overexpressing transgenic plants (TIR1OE and AFB2OE, respectively) (Fig. 2, A and B) and the edited plants (TIR1KO and AFB2KO, respectively) using the CRISPR-Cas9 gene-editing system. One nucleotide (nt) was inserted in *OsTIR1* in each TIR1KO line (Fig. 2C). In the two AFB2KO lines, 1 nt was inserted in one line, and 5 nt were deleted in the other line (Fig. 2D).

We used an individual test and a small population test to evaluate the response of these genetic materials to BPH infestation. In both kinds of assays, TIROE-1 plants died later than wild-type (WT) plants (Fig. 2, E and F), and the survival rates of the TIROE-1 plants were much higher than that of the WT after BPH infestation (Fig. 2G). Similarly, TIROE-2 plants died later than WT plants (Fig. 2, H and I) and had a higher overall survival rate (Fig. 2J). In contrast, TIR1KO-1 (Fig. 2, K and L) and TIR1KO-2 plants (Fig. 2, K and N) died earlier than WT plants, and the respective survival rates were much lower than that of the WT (Fig. 2, M and O). AFB2KO-1 (Fig. 2, P and Q) and AFB2KO-2 plants (Fig. 2, P and S) died earlier than WT plants, and both lines exhibited a much lower survival rate than the WT (Fig. 2, R and T). Thus, the activation of BPH resistance by auxin might be mediated by the OsTIR1 and OsAFB2 receptors.

OsmiR393 modulates auxin signaling posttranscriptionally and BPH resistance negatively

OsTIR1/OsAFB2 are posttranscriptionally modulated by OsmiR393. Two genes encode OsmiR393 in rice, namely, *OsMIR393a* and *OsMIR393b*, with mature OsmiR393a and OsmiR393b being 21 nt and 22 nt long, respectively (http://structuralbiology.cau.edu.cn/PNRD). Both OsmiR393a and OsmiR393b were inhibited in response to BPH feeding (fig. S1, C and D), indicating their possible involvement in BPH resistance.

To study the function of OsmiR393 in BPH resistance, we constructed the *OsMIR393a*- and *OsMIR393b*-overexpressing plants (393aOE and 393bOE, respectively) in the "Nipponbare" (NIP) genetic background. For verification, we detected the expression of mature OsmiR393a and OsmiR393b using miRNA Northern blotting and stem-loop quantitative reverse transcription polymerase chain reaction miRNA assays. OsmiR393a and OsmiR393b were up-regulated in two miR393aOE lines (Fig. 3, A and B) and one 393bOE line (Fig. 3, C and D). Next, we constructed miR393DKO plants in which OsmiR393a and OsmiR393b were knocked out simultaneously. Two lines with different mutations in the mature OsmiR393a and OsmiR393b regions were obtained (Fig. 3E). Accordingly, OsmiR393a and OsmiR393b were both strongly down-regulated in the 393DKO lines (Fig. 3F). Furthermore, in accordance with the posttranscriptional regulation on *OsAFB2* and *OsTIR1* by OsmiR393, in the 393aOE and 393bOE plants, both *OsTIR1* and *OsAFB2* were distinctly down-regulated, whereas, in the 393DKO plants, both genes were up-regulated (Fig. 3G).

In the individual test, the 393aOE-1, 393aOE-2, and 393bOE plants all died much earlier than WT plants (Fig. 4, A to C), indicating a susceptible character to BPH. In the small population test, these three lines died earlier than the WT plants (Fig. 4, D, F, and H), and the survival rates were lower than that of the respective WT (Fig. 4, E, G, and I). Thus, OsmiR393-overexpressing plants were susceptible to BPH.

In the individual test, the 393DKO-1 and 393DKO-2 plants died later than WT plants, indicating that the resistance to BPH was enhanced (Fig. 4, J and K). In the small population test, the 393DKO-1 and 393DKO-2 plants died later than WT plants (Fig. 4, L and N), with much higher survival rates (Fig. 4, M and O). Thus, the OsmiR393a– and OsmiR393b–double-knockout plants had increased resistance to BPH.

During feeding, BPH excretes honeydew. Meanwhile, honeydew is used as a simple measurable indicator of BPH feeding activity (*38*). We determined that a much higher amount of honeydew was excreted by BPH individuals feeding on 393bOE plants than on NIP plants, whereas a greatly reduced amount was excreted by BPH feeding on 393DKO-1 plants (Fig. 4P). Together, these results suggest that the auxin signaling pathway is posttranscriptionally regulated by OsmiR393, which negatively regulates BPH resistance in rice.

OsIAA10 interacts with OsTIR1 to mediate BPH resistance

In mediating auxin signaling, OsTIR1 and OsAFB2 usually interact with OsIAA proteins (*3*). The rice genome includes 31 *OsIAA* genes (*39*). We conducted a yeast two-hybrid (Y2H) assay to test the interaction of most of the OsIAA proteins with OsTIR1 and revealed that many of the OsIAAs interacted with OsTIR1 in yeast system (fig. S2). Next, we examined the expression of these *OsIAA* genes in the 393bOE, 393DKO-1, and WT plants. *OsIAA2*, *OsIAA7*, *OsIAA10*, *OsIAA16*, and *OsIAA24* were down-regulated in 393DKO-1 plants but up-regulated in 393bOE plants (fig. S3; Fig. 5A). A responsive expression assay revealed that these genes were sensitive to BPH infestation. Specifically, expression of *OsIAA10*, *OsIAA16*, and *OsIAA24* showed similar trends in induction in response to BPH infestation (Fig. 5B). Therefore, we inferred that these genes might function in BPH resistance in conjunction with OsTIR1. Given that *OsIAA10* showed the strongest induction response, we focused on *OsIAA10* for further genetic function study.

Various biochemical assays were performed to verify the interaction between OsTIR1 and OsIAA10. In the Y2H assay, the yeast harboring both OsTIR1 and OsIAA10 grew on SD medium deficient of T, L, H, and A (SD/-T-L-HA) supplemented with IAA (fig. S4A). In a luciferase complementation imaging (LCI) assays in *Nicotiana benthamiana* leaves, only the epidermal cells infiltrated with both OsTIR1 and OsIAA10 produced fluorescence (fig. S4B). A bimolecular fluorescence complementation (BiFC) assay further verified the interaction between OsTIR1 and OsIAA10 in planta, while no interaction was detected between OsTIR1 and OsIAA31 (fig. S4C).

Next, we tested the genetic function of *OsIAA10* in resistance to BPH. In individual tests and small population tests, the IAA10KO-1 and IAA10KO-2 plants (*12*) died later than "Zhonghua 11" (ZH11) WT plants (Fig. 5, C, D, and F), with their respective survival rate higher than that of the WT in the small population test (Fig. 5, E and G). We constructed *OsIAA10*-overexpressing lines and chose

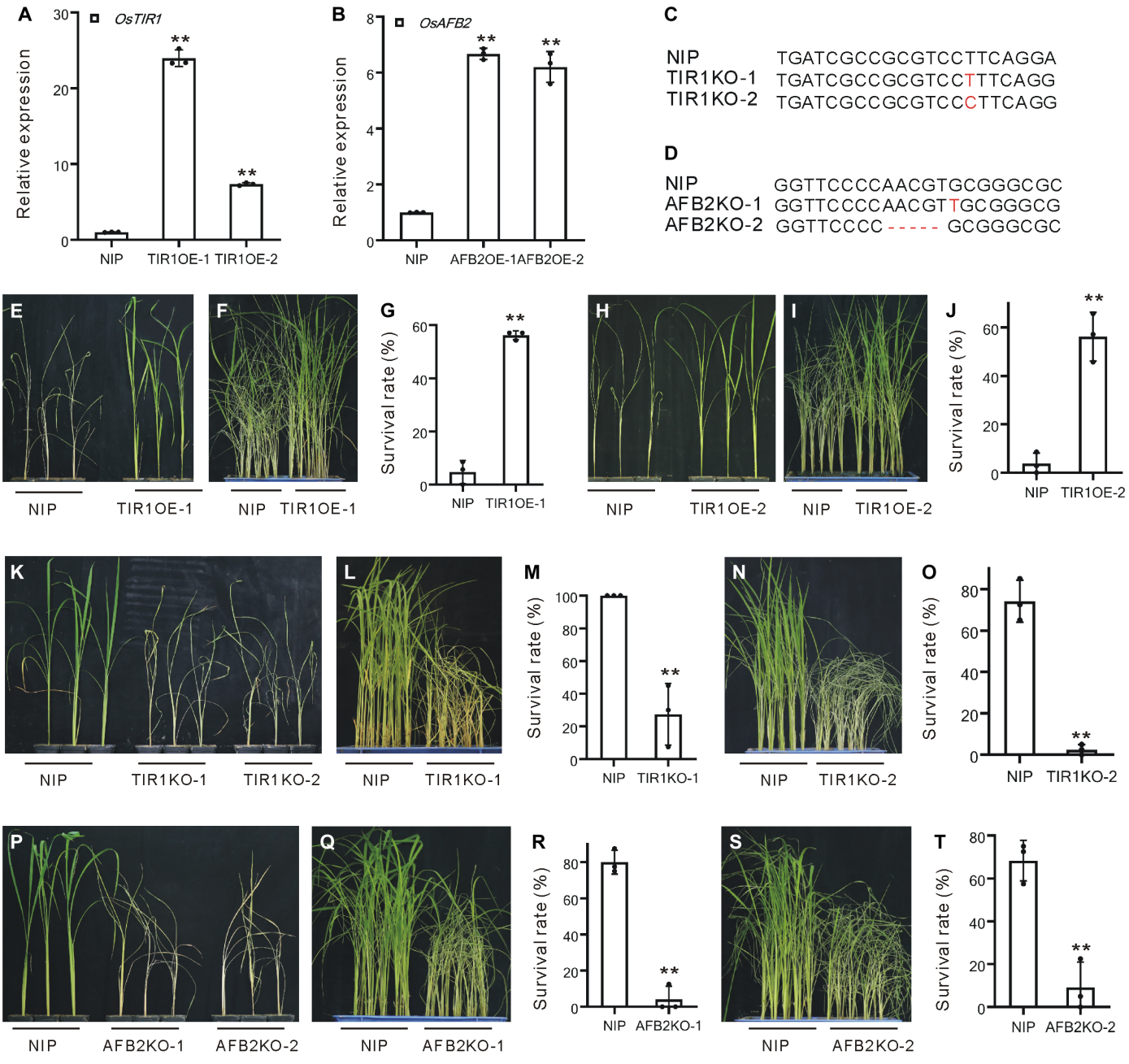

Fig. 2. BPH resistance of the TIR1OE, TIR1KO, and AFB2KO plants. (**A**) Expression of *OsTIR1* gene in the TIR1OE lines and NIP plants. Data are means ± SD ($n = 3$). (**B**) Expression of *OsAFB2* gene in the AFB2OE lines and NIP plants. Data are means ± SD ($n = 3$). (**C**) Edited sites (marked red) in the *OsTIR1* nucleotide sequence for the TIR1KO lines. (**D**) Edited sites (marked red) in the *OsAFB2* nucleotide sequence for the AFB2KO lines. (**E**) Individual test of the TIR1OE-1 and wild-type (WT) plants. (**F**) Small population test of the TIR1OE-1 and WT plants. (**G**) Survival rates of the plants in (F). Data are means ± SD ($n = 3$). (**H**) Individual test of the TIR1OE-2 and WT plants. (**I**) Small population test of the TIR1OE-2 and WT plants. (**J**) Survival rates of the plants in (I). Data are means ± SD ($n = 3$). (**K**) Individual test of the TIR1KO-1, TIR1KO-2, and WT plants. (**L**) Small population test of the TIR1KO-1 and WT plants. (**M**) Survival rates of the plants in (L). Data are means ± SD ($n = 3$). (**N**) Small population test of the TIR1KO-2 and WT plants. (**O**) Survival rates of the plants in (N). Data are means ± SD ($n = 3$). (**P**) Individual test of the AFB2KO-1, AFB2KO-2 and WT plants. (**Q**) Small population test of the AFB2KO-1 and WT plants. (**R**) Survival rates of the plants in (Q). Data are means ± SD ($n = 3$). (**S**) Small population test of the AFB2KO-2 and WT plants. (**T**) Survival rates of the plants in (S). Data are means ± SD ($n = 3$). Student's *t* test was carried out in [(A), (B), (G), (J), (M), (O), (R), and (T)] to compare with NIP, respectively (**$P < 0.01$).

two lines, IAA10OE-1 and IAA10OE-2, for testing (fig. S5). In individual tests and small population tests, the IAA10OE-1 and IAA10OE-2 plants died earlier than WT plants (Fig. 5, H, I, and K), and their respective survival rates were lower than that of the WT in the small population test (Fig. 5, J and L). Thus, *OsIAA10* negatively regulated BPH resistance.

OsARF12 acts downstream of OsTIR1/OsIAA10 to mediate BPH resistance

Under auxin deficiency, IAA proteins often combine with ARFs and inhibit the function of these ARFs. When sufficient auxin is available, ARFs are released from the combination with IAAs to regulate downstream genes (*3*). Twenty-five OsARF proteins are recorded in

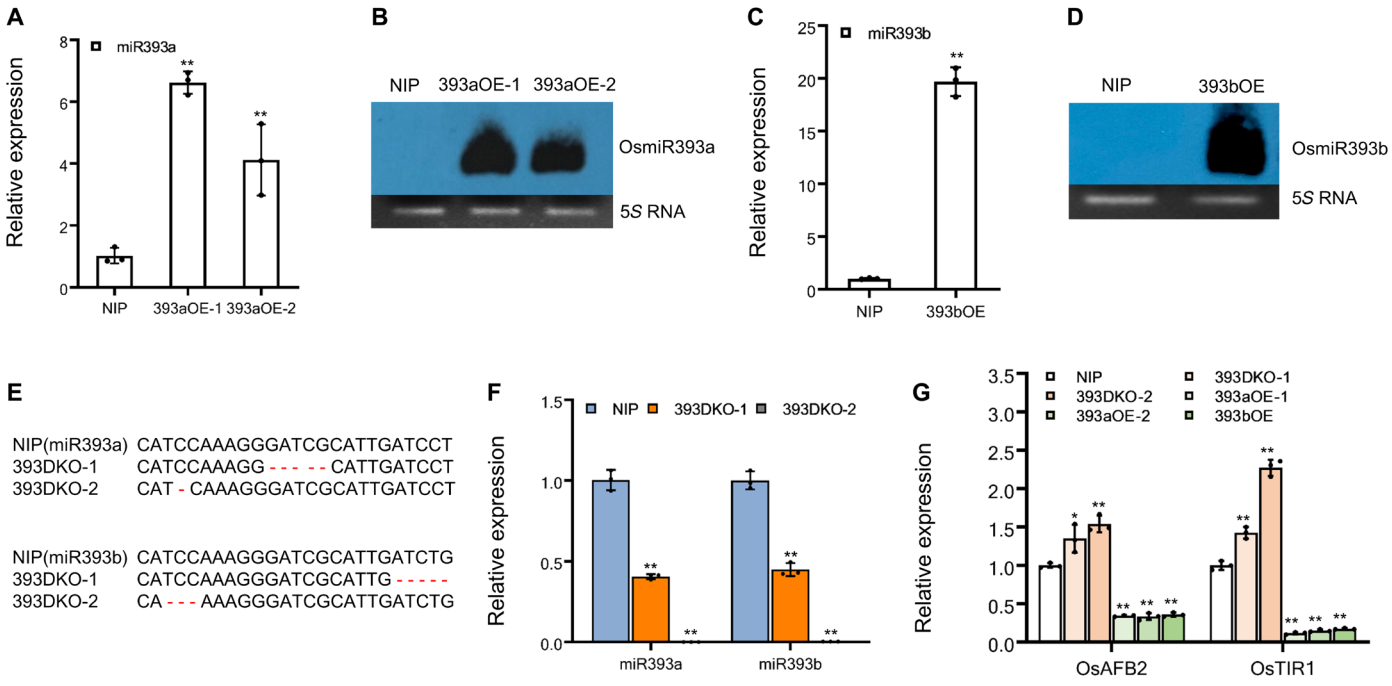

Fig. 3. Verification and detection of 393aOE, 393bOE, and 393DKO plants. (**A**) Stem-loop quantitative reverse transcription polymerase chain reaction (qRT-PCR) miRNA assay of OsmiR393a in the 393aOE and WT plants. Data are means ± SD ($n = 3$). (**B**) miRNA Northern blotting of OsmiR393a in the 393aOE and WT plants. (**C**) Stem-loop qRT-PCR miRNA assay of OsmiR393b in the 393bOE and WT plants. Data are means ± SD ($n = 3$). (**D**) miRNA Northern blotting of OsmiR393b in the 393bOE and WT plants. (**E**) Edited sites (marked red) in the OsmiR393a and OsmiR393b nucleotide sequence for the two lines of 393DKO plants. In 393DKO-1, there is a 70–base pair (bp) deletion in the miR393b genomic region. (**F**) Stem-loop qRT-PCR miRNA assay of OsmiR393a and OsmiR393b in the 393DKO and WT plants. Data are means ± SD ($n = 3$). (**G**) Expression of *OsAFB2* and *OsTIR1* genes in the 393aOE, 393bOE, 393DKO, and WT plants. Data are means ± SD ($n = 3$). Student's *t* test was carried out in [(A), (C), (F), and (G)] to compare with NIP, respectively (*$P < 0.05$; **$P < 0.01$).

rice, and many of them have been reported to interact with OsIAA10 to mediate resistance to the rice RDV (*12*). For verification, in an Y2H assay, yeast harboring both OsIAA10 and OsARF12 grew well on the SD/-T-L-H-A medium (Fig. 6A). In addition, the interaction between OsIAA10 and OsARF12 was verified in LCI (Fig. 6B), BiFC (Fig. 6C), and co-immunoprecipitation (co-IP) assays (Fig. 6D). All these biochemical assays indicated that OsIAA10 interacted with OsARF12 in vitro and in vivo. Thus, the OsTIR1/OsIAA10 module might function through OsARF12 to mediate downstream auxin signaling.

Next, we tested the genetic function of *OsARF12* gene in BPH resistance. First, we tested the expression of *OsARF12* upon BPH infestation. *OsARF12* was rapidly induced by BPH infestation (fig. S6A). We obtained two ARF12KO lines and two ARF12OE lines as gifts (*12*). In individual tests, all ARF12KO-1 (Fig. 6E) and ARF12KO-2 (Fig. 6F) plants died earlier than the ZH11 WT plants. In small population tests, both lines died earlier than ZH11 plants (Fig. 6, G and I), with the respective survival rates much lower than that of ZH11 plants (Fig. 6, H and J). In both types of BPH resistance tests, ARF12OE-1 and ARF12OE-2 plants died later than ZH11 plants (Fig. 6, K to N), with the respective survival rates higher than that of ZH11 plants (Fig. 6, M and O), indicating that resistance to BPH was enhanced in both lines. In addition, we obtained ARF12OE lines in the NIP genetic background (designated ARF12OEn) and confirmed that the ARF12OEn plants were more resistant to BPH than NIP WT plants (fig. S6, B and C). In detection of honeydew excretion, a greater amount of honeydew was excreted by BPH individuals feeding on ARF12KO-1 plants than on ZH11 plants, whereas the amount was much less on the ARF12OE-1 plants (Fig. 6P). Therefore, *OsARF12* positively regulated BPH resistance.

Simultaneously, in the "Kasalath" genetic background, we generated a 393DKOk line (fig. S7A) using the CRISPR-Cas9 gene-editing system and obtained an ARF12KOk line as gift (fig. S7B) (*40*). In an individual test, 393DKOk plants died later than the Kasalath WT plants (fig. S8, A and B), indicative of resistance to BPH similar to that of 393DKO in NIP background. Meanwhile, in an individual test, the ARF12KOk plants died earlier than the WT plants (fig. S8, C and D), indicating susceptibility to BPH similar to that of ARF12KO in ZH11 background. To test the genetic interaction between OsmiR393 and *OsARF12*, we crossed the ARF12KOk and 393DKOk plants. In the cross plant 393DKOk/ARF12KOk, the edited OsmiR393a, OsmiR393b, and OsARF12 genomic regions were successfully inherited from the parents (fig. S7C). In an individual test, the cross plants 393DKOk/ARF12KOk were more susceptible to BPH than the 393DKOk plants, with a status similar to that of the WT plants (Fig. 6Q). Therefore, the BPH resistance of the 393DKOk plants was dependent on *OsARF12* gene.

OsARF12 genetically activates the downstream gene *OsRbohB*

Nine genes encode Rbohs in rice, which account for the main source of H_2O_2 production upon an adverse condition. We examined whether these *OsRbohs* are involved in BPH resistance. The expression of seven genes was severely influenced by BPH infestation, with the induction of *OsRbohB* being the most marked change (Fig. 7A). We thus investigated the function of *OsRbohB* in BPH resistance by testing the BPH resistance of the *osrbohB* mutant (*41*). In an

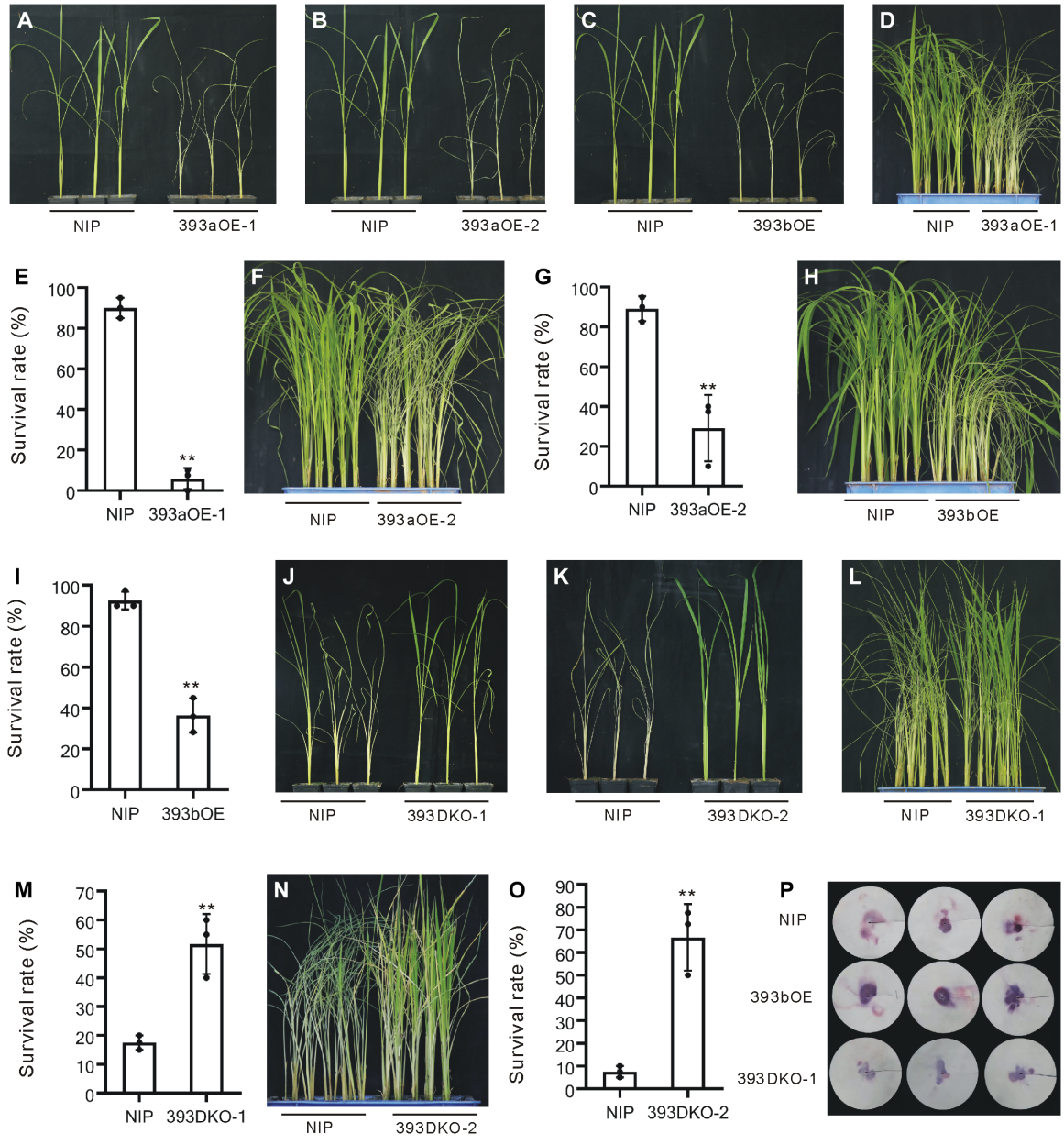

Fig. 4. BPH resistance of the 393aOE, 393bOE, and 393DKO plants compared with WT plants. (**A**) Individual test of the 393aOE-1 and NIP plants. (**B**) Individual test of the 393aOE-2 and NIP plants. (**C**) Individual test of the 393bOE and NIP plants. (**D**) Small population test of the 393aOE-1 and NIP plants. (**E**) Survival rates of the plants in (**D**). Data are means ± SD ($n = 3$). (**F**) Small population test of the 393aOE-2 and NIP plants. (**G**) Survival rates of the plants in (F). Data are means ± SD ($n = 3$). (**H**) Small population test of the 393bOE and NIP plants. (**I**) Survival rates of the plants in (H). Data are means ± SD ($n = 3$). (**J**) Individual test of the 393DKO-1 and NIP plants. (**K**) Individual test of the 393DKO-2 and NIP plants. (**L**) Small population test of the 393DKO-1 and NIP plants. (**M**) Survival rates of the plants in (L). Data are means ± SD ($n = 3$). (**N**) Small population test of the 393DKO-2 and NIP plants. (**O**) Survival rates of the plants in (N). Data are means ± SD ($n = 3$). (**P**) Honeydew content in the 393bOE, 393DKO-1, and NIP plants after BPH infestation for 48 hours. Honeydew was excreted on filter paper. The size of the honeydew area and the intensity of the honeydew color correspond to the BPH feeding activity. Student's *t* test was carried out in [(E), (G), (I), (M), and (O)] to compare with NIP, respectively (**$P < 0.01$).

individual test (fig. S9, A and B) and a small population test (fig. S9, C and D), the *osrbohB* mutant plants died earlier than WT plants, and the survival rate was much lower than that of the WT plants (fig. S9E). Before BPH infestation, H_2O_2 content in the *osrbohB* mutant was lower than that in NIP, as indicated by 3,3′-diaminobenzidine (DAB) staining and H_2O_2 content measurement (Fig. 7, B and C). BPH infestation activated H_2O_2 accumulation in the *osrbohB* mutant and NIP plants, but the activation degree in the *osrbohB* mutant plants was not comparable to that in NIP plants (Fig. 7, B and D). Thus, *OsRbohB* gene positively regulated BPH resistance through H_2O_2 accumulation.

Next, we examined whether OsARF12 could directly regulate *OsRbohB* transcription. We first detected the transcriptional activation effect of OsARF12 using the GAL4 system. The full-length coding

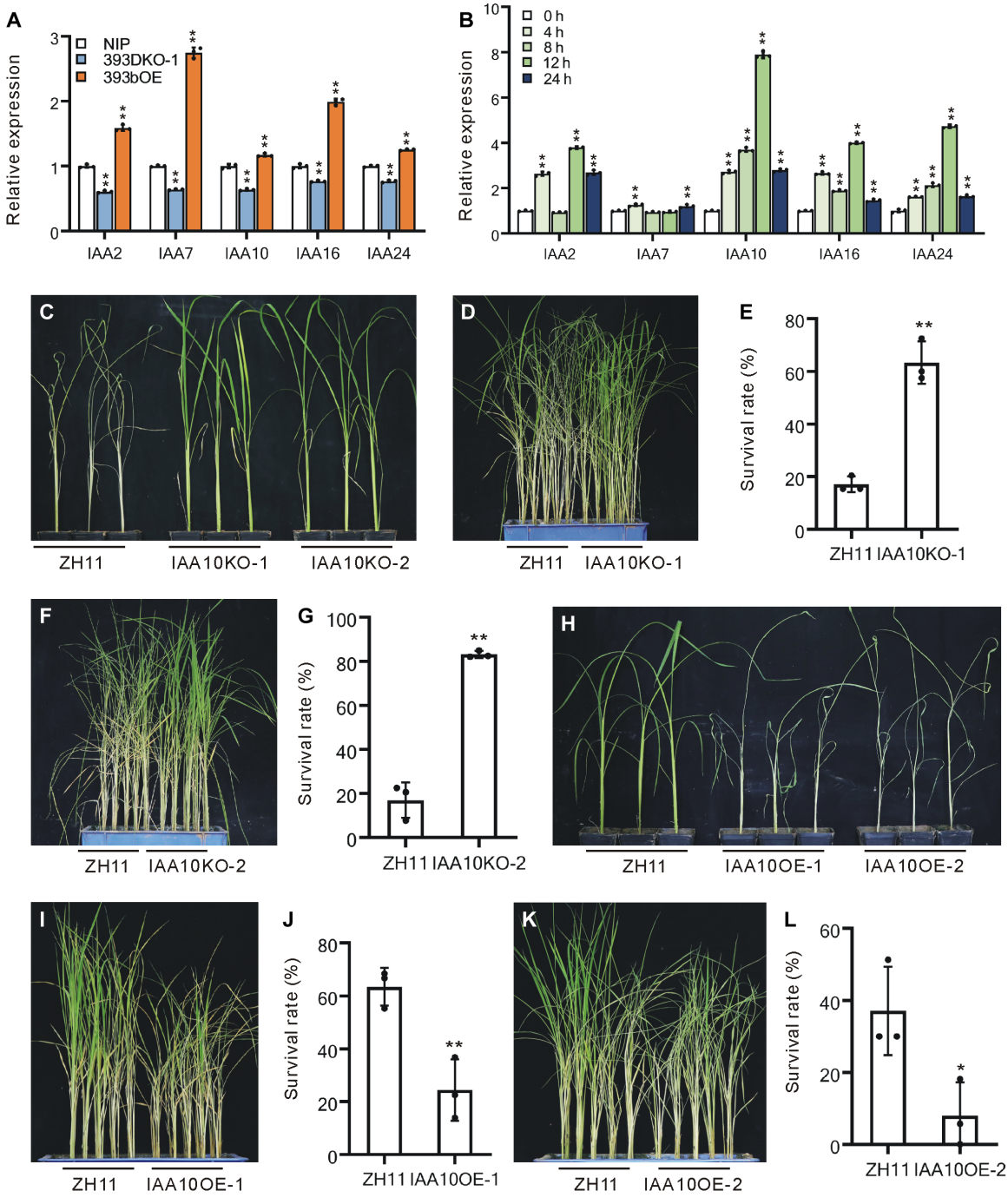

Fig. 5. Expression of certain *OsIAA* genes and genetic function analysis of *OsIAA10*. (**A**) Expression of *OsIAA2*, *OsIAA7*, *OsIAA10*, *OsIAA16*, and *OsIAA24* genes in the 393DKO-1, 393bOE, and WT NIP plants. Data are means ± SD ($n = 3$). Student's *t* test was carried out to compare with NIP (**$P < 0.01$). (**B**) Expression of *OsIAA2*, *OsIAA7*, *OsIAA10*, *OsIAA16*, and *OsIAA24* genes upon BPH infestation. Data are means ± SD ($n = 3$). Student's *t* test was carried out to compare with 0 hours (**$P < 0.01$). (**C**) Individual test of the IAA10KO-1 and IAA10KO-2 lines and WT ZH11 plants. (**D**) Small population test of the IAA10KO-1 and WT ZH11 plants. (**E**) Survival rates of the plants in (D). Data are means ± SD ($n = 3$). (**F**) Small population of the IAA10KO-2 and WT ZH11 plants. (**G**) Survival rates of the plants in (F). Data are means ± SD ($n = 3$). (**H**) Individual test of the IAA10OE-1 and IAA10OE-2 lines and WT ZH11 plants. (**I**) Small population of the IAA10OE-1 and WT ZH11 plants. (**J**) Survival rates of the plants in (I). Data are means ± SD ($n = 3$). (**K**) Small population test of the IAA10OE-2 and ZH11 WT plants. (**L**) Survival rates of the plants in (K). Data are means ± SD ($n = 3$). Student's *t* test was carried out in [(E), (G), (J), and (L)] to compare with ZH11, respectively (*$P < 0.05$; **$P < 0.01$). h, hours.

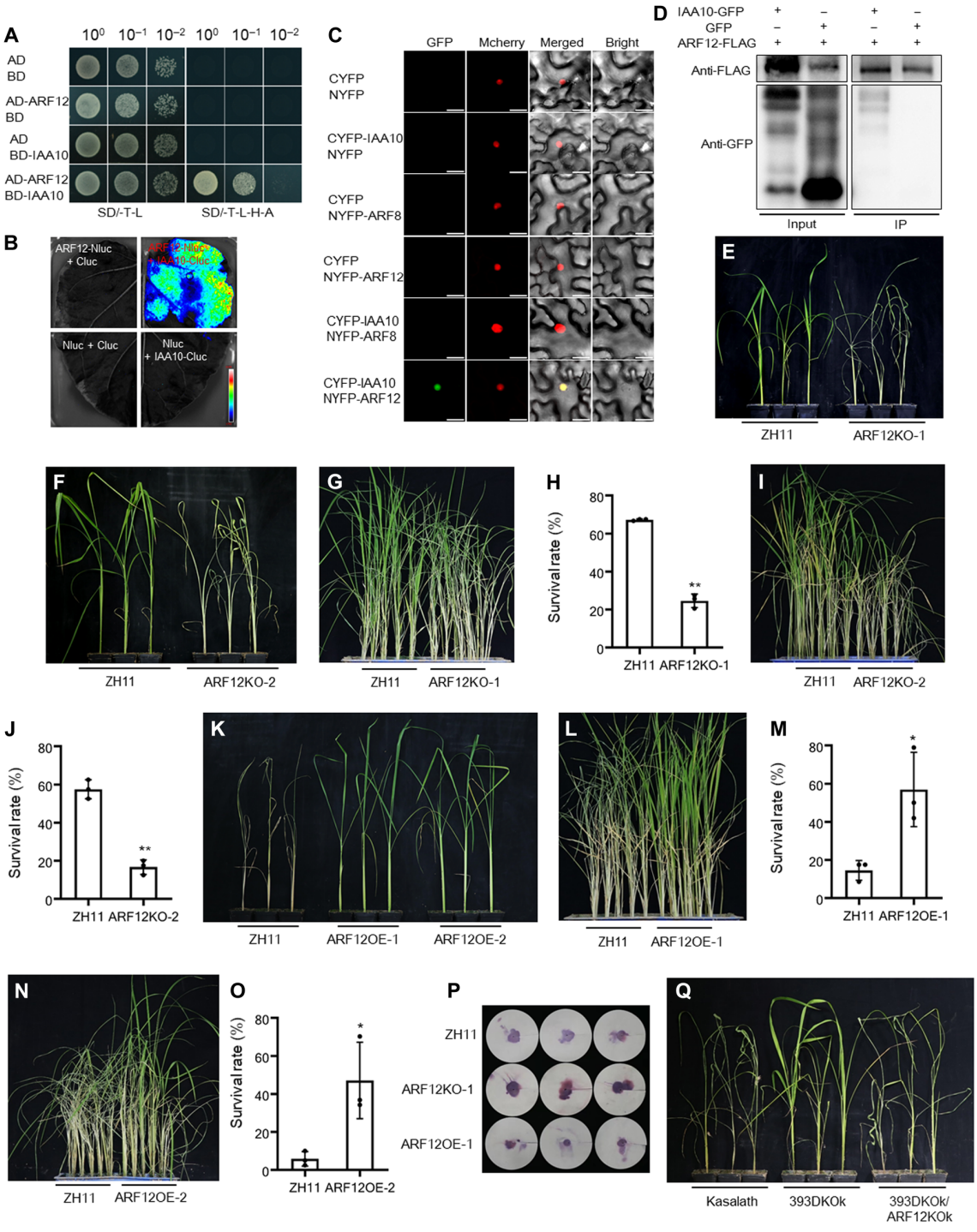

Fig. 6. Interaction verification of OsIAA10 and OsARF12, and genetic function analysis of *OsARF12*. (**A**) Y2H assay between OsARF12 and OsIAA10 proteins. (**B**) LCI assay of the interaction between OsARF12 and OsIAA10. (**C**) BiFC assay of the OsARF12 and OsIAA10 proteins. The couple of OsIAA10 and OsARF8 was used as negative control. Scale bars, 30 μm. (**D**) Co-immunoprecipitation (Co-IP) assay of the OsARF12 and OsIAA10 proteins. (**E**) Individual test of the ARF12KO-1 and WT plants. (**F**) Individual test of the ARF12KO-2 and WT plants. (**G**) Small population test of the ARF12KO-1 and WT plants. (**H**) Survival rates of the plants in (G). Data are means ± SD ($n = 3$). (**I**) Small population test of the ARF12KO-2 and WT plants. (**J**) Survival rates of the plants in (I). Data are means ± SD ($n = 3$). (**K**) Individual test of the ARF12OE-1, ARF12OE-2, and WT plants. (**L**) Small population test of the ARF12OE-1 and WT plants. (**M**) Survival rates of the plants in (L). Data are means ± SD ($n = 3$). (**N**) Small population test of the ARF12OE-2 and WT plants. (**O**) Survival rates of the plants in (N). Data are means ± SD ($n = 3$). (**P**) Honeydew content in the ARF12KO-1, ARF12OE-1, and ZH11 plants after BPH infestation for 48 hours. Honeydew was excreted on filter paper. The size of the honeydew area and the intensity of the honeydew color correspond to the BPH feeding activity. (**Q**) Individual test of Kasalath, 393DKOk, and the 393DKOk/ARF12KOk cross plants. Student's *t* test was carried out in [(H), (J), (M), and (O)] to compare with ZH11, respectively (*$P < 0.05$; **$P < 0.01$).

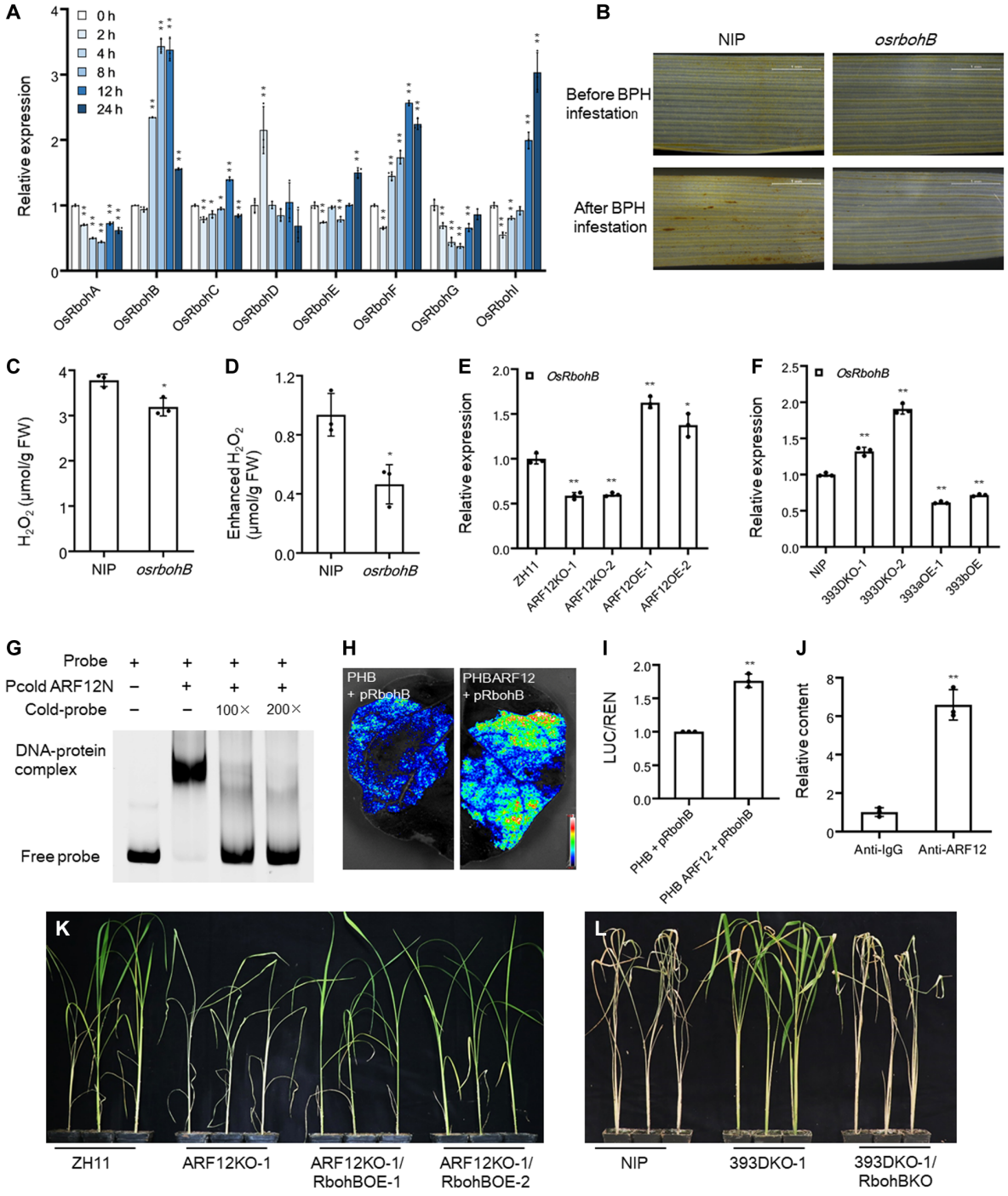

Fig. 7. Transcriptional regulation of *OsRbohB* by OsARF12, genetic function analysis of *OsRbohB*, and its genetic relationship with *OsARF12* and OsmiR393. (**A**) Expression of *OsRboh* genes under BPH infestation. Data are means ± SD ($n = 3$). Student's *t* test was carried out to compare with 0 hours (*$P < 0.05$; **$P < 0.01$). (**B**) 3,3′-Diaminobenzidine (DAB) staining of H_2O_2 in leaves of the *osrbohB* mutant and NIP plants before and after BPH infestation. (**C**) H_2O_2 content in the *osrbohB* mutant and NIP plants before BPH infestation. Data are means ± SD ($n = 3$). (**D**) Increase in H_2O_2 content in the *osrbohB* mutant and NIP plants after BPH infestation. Data are means ± SD ($n = 3$). (**E**) Analysis of the mRNA level of *OsRbohB* in the ARF12OE, ARF12KO, and WT plants. Data are means ± SD ($n = 3$). (**F**) Relative abundance of *OsRbohB* mRNA in the 393aOE-1, 393bOE, 393DKO-1, 393DKO-2, and WT plants. Data are means ± SD ($n = 3$). (**G**) EMSA of the N terminus of the OsARF12 (ARF12N, 1 to 247 amino acids) and the promoter of *OsRbohB*. The promoter region for assay was indicated in fig. S11. (**H**) Dual-luciferase (LUC) assay of the OsARF12 protein and the promoter region of *OsRbohB*. (**I**) LUC/REN ration in (H). Data are means ± SD ($n = 3$). (**J**) Chromatin immunoprecipitation (ChIP) assay of ARF12OE plants and the anti-ARF12 antibody and the anti-IgG antibody was used as control. The promoter region for assay was indicated in fig. S11. Data are means ± SD ($n = 3$). (**K**) Individual test of the ARF12KO-1/RbphBOE-1, ARF12KO-1/RbohBOE-2, ARF12KO-1, and WT plants. (**L**) Individual test of the 393DKO-1/RbohBKO, 393DKO-1, and WT plants. Student's *t* test was carried out in [(C) to (F), (I), and (J)] (*$P < 0.05$; **$P < 0.01$). h, hours.

sequence of Os*ARF12* was fused to *GAL4BD* for subsequent expression under the control of the 35*S* promoter and used as an effector, with GAL4BD serving as the negative control and GAL4BD-VP16 serving as the positive control (fig. S10A). The 35*S* promoter, six tandem repeats of upstream active sequence (UAS) (CGGAGTACTGTCCTCCGAG), which is the binding site for GAL4BD, and a TATA-Box were fused to the *LUC* gene to form 35*S*-6×UAS-TATA-LUC as the reporter (fig. S10A). When expressed in the *N. benthamiana* leaves, GAL4BD-ARF12 showed stronger luciferase activity than GAL4BD (fig. S10, B and C), indicating that OsARF12 has a transcriptional activation effect.

In an expression assay, *OsRbohB* gene was up-regulated in the ARF12OE plants but down-regulated in the ARF12KO plants (Fig. 7E), indicating that OsARF12 might regulate *OsRbohB*. Furthermore, *OsRbohB* gene was up-regulated in the 393DKO-1 and 393DKO-2 plants but down-regulated in the 393aOE and 393bOE plants (Fig. 7F), indicating possible involvement of *OsRbohB* gene in OsmiR393-mediated signaling. The binding motif for ARF transcription factors is AuxRE TGTCT(A, C)C/GA(T, G)GACA (*12*). Two AuxRE motifs are located in the 2-kb promoter of *OsRbohB* (fig. S11). We performed an electrophoretic mobility shift assay (EMSA) and verified that the N terminus of OsARF12, which contains the DNA binding domain, could bind to the fragment of *OsRbohB* promoter (Fig. 7G). Furthermore, in a dual-luciferase (LUC) assay, OsARF12 could activate the expression of *OsRbohB* promoter (Fig. 7H), which was verified by the LUC/REN ratio (Fig. 7I). Moreover, using the ARF12OE plants, we conducted a chromatin immunoprecipitation (ChIP) assay and confirmed that the fragment of *OsRbohB* promoter was enriched in chromosomal DNA precipitated by *anti-ARF12 antibodies* (Fig. 7J). Together, we proved that OsARF12 could directly activate the expression of *OsRbohB* in rice.

To further verify that *OsRbohB* gene functions in the OsmiR393/OsTIR1-OsIAA10-OsARF12 pathway to mediate BPH resistance, we overexpressed *OsRbohB* in the ARF12KO-1 background. In the transgenic ARF12KO-1/RbohBOE plants, *OsARF12* was down-regulated (fig. S12A), whereas *OsRbohB* gene was up-regulated (fig. S12B), compared with the respective expression levels in ZH11. In the BPH resistance test, after infestation by BPH for 7 days, the ARF12KO-1 plants died, whereas ZH11 plants and the two lines of the ARF12KO-1/RbohBOE plants remained alive (Fig. 7K). Therefore, the BPH susceptibility of the ARF12KO-1 plants was complemented by *OsRbohB* overexpression.

To further detect the genetic interaction between OsmiR393 and *OsRbohB* gene, we knocked out *OsRbohB* in the 393DKO-1 plants through genetic transformation. The resulting 393DKO-1/RbohBKO plants had a single-base "A" insertion in the *OsRbohB* gene region (fig. S12C). In an individual test, 393DKO-1/RbohBKO plants were more susceptible to BPH in comparison with 393DKO-1 plants, indicating that the resistance of 393DKO-1 plants was dependent on *OsRbohB* gene (Fig. 7L).

Involvement of ROS in OsmiR393/OsTIR1 signaling–mediated BPH resistance

ROS are broadly involved in the downstream signaling mechanism in various plant defense response. ROS mediate the function of *OsARF12* in resistance against RDV (*12*), and OsRboh-mediated ROS concentrations play important roles in defense against rice black streaked dwarf virus (RBSDV) (*42*). To verify whether ROS are involved in BPH resistance, we first treated the rice plants with H_2O_2 before BPH infestation. The plants pretreated with H_2O_2 showed superior survival after BPH infestation, with the survival rate increasing with increased H_2O_2 concentration (fig. S13, A and B). Next, we tested the H_2O_2 content in the typical BPH-resistant rice cultivar RHT and the susceptible cultivar 9311. The basal H_2O_2 content in RHT was slightly higher than that in 9311 (Fig. 8, A and B). Whereas, under BPH infestation, the H_2O_2 content in the RHT plants was greatly enhanced, while it was also enhanced in 9311 plants, only that the elevation was not comparable to that in RHT (Fig. 8, A and C). Next, we measured the H_2O_2 content in the OsmiR393-overexpressing and gene-edited plants. Although the basal H_2O_2 content in the 393bOE plants was similar to that in NIP plants, it was much higher in the 393DKO-1 plants than in NIP plants (Fig. 8, D and E). Under BPH infestation, the H_2O_2 contents in all tested plants were increased (Fig. 8D), with the promotion in the 393DKO-1 much higher than that in NIP plants, while that in the 393bOE plants lower than that in NIP (Fig. 8F). Next, we measured the H_2O_2 content in *OsARF12*-overexpressing and gene-edited plants before and after BPH infestation. In the ARF12OE plants, the basal H_2O_2 content was higher than that in ZH11 plants, while that in the ARF12KO plants was lower (Fig. 8, G and H). Under BPH infestation, the H_2O_2 contents in the ARF12OE, ARF12KO, and ZH11 plants were all increased (Fig. 8G). In addition, the increase of H_2O_2 content in the ARF12OE plants was higher than that in ZH11 plants (Fig. 8I).

Next, we examined whether chitin could induce ROS production in the OsmiR393/OsTIR1-OsIAA-OsARF12 pathway. In the 393DKO plants (Fig. 8J), TIR1OE plants (Fig. 8K), IAA10KO plants (Fig. 8L), and the ARF12OE plants (Fig. 8M), chitin-induced ROS production was enhanced, whereas, in the 393aOE, 393bOE plants (Fig. 8J), TIR1KO plants (Fig. 8K), IAA10OE plants (Fig. 8L), and the ARF12KO plants (Fig. 8M), ROS production was compromised. Thus, ROS activation was extensively involved in the OsmiR393/OsTIR1-OsIAA10-OsARF12-OsRbohB signaling pathway, and this involvement was tightly associated with BPH resistance.

Furthermore, we tested the association between BPH resistance and ROS in consistency with the genetic relationship between OsARF12 and *OsRbohB*, OsmiR393 and *OsRbohB*, and OsmiR393 and OsARF12. We have proved that the BPH susceptibility of the ARF12KO-1 plants was complemented by *OsRbohB* overexpression (Fig. 7K), and, in consistency, the low ROS content in the ARF12KO-1 plants was recovered (Fig. 8N). Also, the 393DKO-1/RbohBKO plants were more susceptible to BPH, in comparison with the 393DKO-1 plants (Fig. 7L), and, consistently, the chitin-induced ROS production was compromised in the 393DKO-1/RbohBKO plants compared with that in the 393DKO-1 plants (Fig. 8O). In addition, we have proved that OsmiR393 genetically regulates *OsARF12* to mediate BPH resistance (Fig. 6Q). We further evaluated whether the ROS content was underlying this genetic association. As revealed, the chitin-induced ROS production was compromised in the 393DKOk/ARF12KOk plants compared with that in the 393DKOk plants (Fig. 8P).

DISCUSSION

Phytohormones play central roles in balancing plant growth and survival against diverse biotic and abiotic stresses. Among the various phytohormones, inhibition of auxin is usually adopted by plants in defense and, therefore, is regarded as a negative regulator of innate immunity (*43*). However, pathogens have evolved counter-defense strategies to manipulate phytohormone signaling pathways, such as

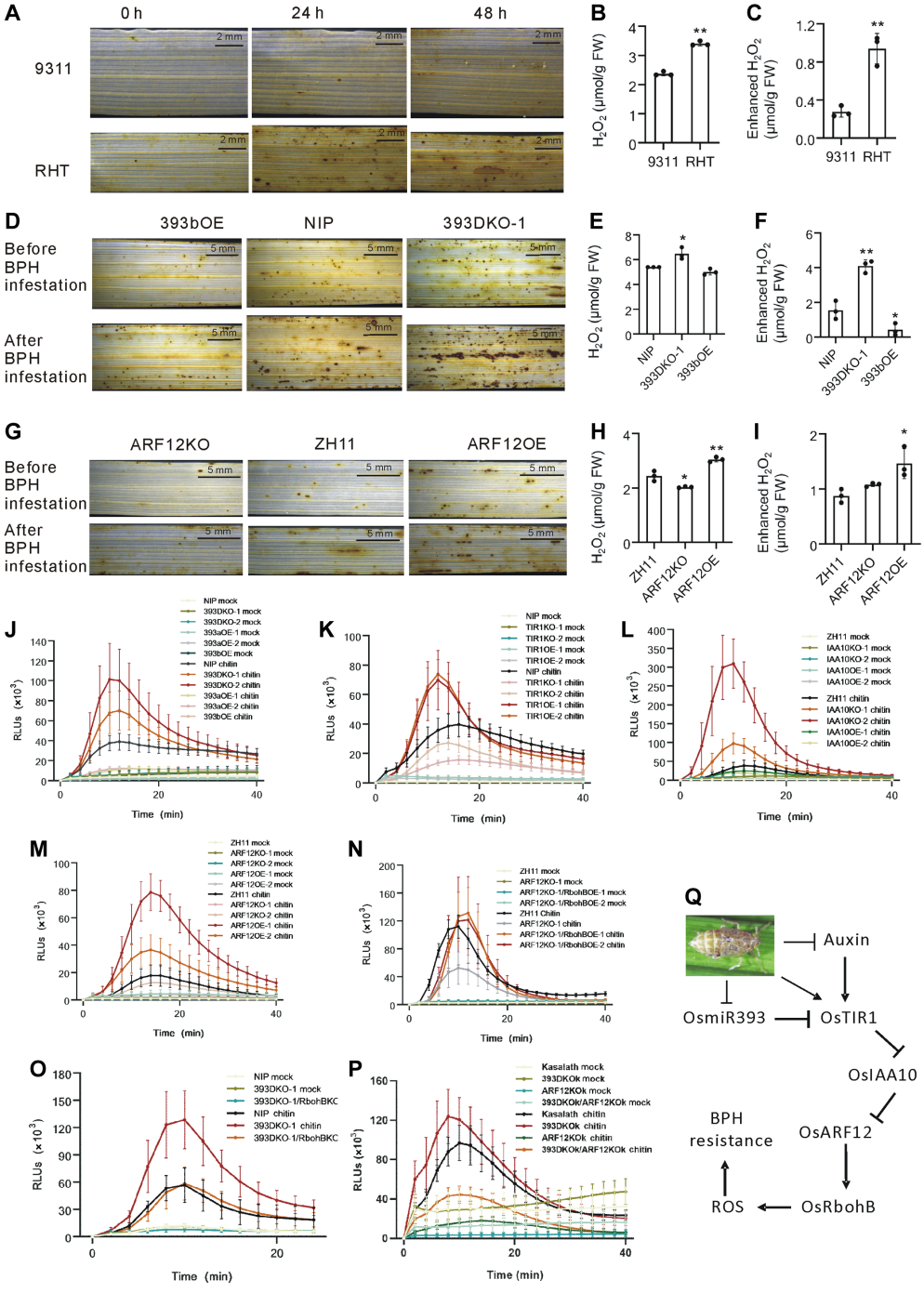

Fig. 8. ROS content in the OsmiR393/TIR1-OsIAA10-OsARF12–OsRbohB pathway in response to BPH infestation. (**A**) DAB staining of RHT and 9311 leaves before and after BPH infestation. (**B**) H_2O_2 content in RHT and 9311 plants before BPH infestation. Data are means ± SD ($n = 3$). (**C**) Increase in H_2O_2 content in RHT and 9311 plants after BPH infestation. Data are means ± SD ($n = 3$). (**D**) DAB staining of leaves of the 393bOE, 393DKO-1, and WT plants before and after BPH infestation. (**E**) H_2O_2 content in the 393bOE, 393DKO-1, and WT plants before BPH infestation. Data are means ± SD ($n = 3$). (**F**) Increase in H_2O_2 content in the 393bOE, 393DKO-1, and WT plants after BPH infestation. Data are means ± SD ($n = 3$). (**G**) DAB staining of leaves of the ARF12OE, ARF12KO, and WT rice plants before and after BPH infestation. (**H**) H_2O_2 content in the ARF12OE, ARF12KO, and WT plants before BPH infestation. Data are means ± SD ($n = 3$). (**I**) Increase in H_2O_2 content in the ARF12OE, ARF12KO, and WT plants after BPH infestation. Data are means ± SD ($n = 3$). (**J** to **M**) Chitin-induced ROS burst in corresponding plant lines. (**N**) Chitin-induced ROS burst in the ARF12KO-1/RbohBOE-1, ARF12KO-1/RbohBOE-2, ARF12KO-1, and WT plants. (**O**) Chitin-induced ROS burst in the 393DKO-1/RbohBKO, 393DKO-1, and WT plants. Data are means ± SD. (**P**) Chitin-induced ROS burst in the 393DKOk/ARF12KOk, 393DKOk, ARF12KOk, and WT plants. In all the tests for chitin-induced ROS burst, Data are means ± SD ($n = 8$, biologically independent samples). (**Q**) Schematic illustration of the OsmiR393/OsTIR1-OsIAA10-OsARF12-OsRbohB pathway in mediating BPH resistance through cross-talk between auxin and ROS. Student's *t* test was carried out in [(B) and (C)] to compare with 9311, in [(E) and (F)] to compare with NIP, and in [(H) and (I)] to compare with ZH11, respectively (*$P < 0.05$; **$P < 0.01$). h, hours.

biosynthesis, signaling, and transport, to dampen immunity and promote virulence (*44*, *45*). As examples, miR393-mediated suppression of auxin signaling in resistance has been, respectively, illustrated in *Arabidopsis* and cotton (*46*, *47*). In the present study, we demonstrated that auxin signaling plays a role in activation of plant defense against BPH. Application of exogenous auxin at a low concentration resulted in enhanced resistance to BPH (Fig. 1A). Consistent with this finding, mutation of either auxin receptor, OsAFB2 or OsTIR1, caused susceptibility to BPH (Fig. 2, K to T). Furthermore, overexpression of both OsmiR393a and OsmiR393b, the miRNAs that target *OsAFB2* and *OsTIR1*, renders the plants more vulnerable to BPH infestation (Fig. 4, A to I). Consistently, *OsIAA10*-overexpressing (Fig. 5, H to L) and *OsARF12*-knockout plants (Fig. 6, E to J) were more vulnerable to BPH infestation. In contrast, knockout of OsmiR393a and OsmiR393b (Fig. 4, J to O) and *OsIAA10* (Fig. 5, C to G) and overexpression of *OsTIR1* (Fig. 2, E to J) and *OsARF12* (Fig. 6, K to O) resulted in stronger resistance to BPH than that of the WT. These results illustrate that auxin is closely associated with rice resistance to BPH, and a low concentration of auxin activates the plant signaling pathways involved in the response to BPH infestation. Consistently, repression of *OsTIR1* by OsmiR393 overexpression increases rice susceptibility to RBSDV (*42*). Infection by RDV interferes with auxin signaling through blocking the interaction between OsIAA10 and OsTIR1 and thus inhibiting OsIAA10 degradation (*10*). The tomato spotted wilt virus (TSWV) shows a deliberate attempt to disrupt plant growth and to promote its spread in sensitive cultivars mediated by the miR167a-ARF8 module (*48*). Moreover, several types of phytohormone receptors, including auxin, JA, and strigolactone receptors, are directly targeted by the effector of TSWV to inhibit signaling and promote virulence. However, this interference is recognized by a plant NLR protein as a counter-virulence strategy to activate immunity (*43*). Therefore, the auxin signaling pathway is a battlefield that is generally fought over by both biotic factors and plants.

ROS signaling is essential for plant growth and development and in response to different abiotic and biotic stresses, which assist the plant to acclimate and adapt to cellular metabolic perturbation and environmental stimuli (*18*, *49*, *50*). To ensure efficient ROS signaling, cells are equipped with the machinery to locally synthesize ROS to initiate cellular responses on one hand and to scavenge or transport ROS to prevent them from reaching damaging level on the other hand. ROS are broadly involved in the downstream signaling of PTI. In *Arabidopsis*, ROS signaling functions in stomatal immunity; the flg22 peptide is perceived by a co-receptor complex that can activate BOTRYTIS-INDUCED KINASE1 (BIK1), which, in turn, activates RbohD through phosphorylation (*51*). Similarly, in rice, OsRACK1A is recognized by the effector of the false smut fungus, *Ustilaginoidea virens*, UvCBP1, which disturbs the interaction between OsRACK1A and OsRbohB, whereas OsRACK1A promotes OsRbohB-mediated ROS production and confers resistance (*52*). The importance of ROS in BPH resistance was revealed in the present study. First, ROS was proved to be a responsive factor to BPH infestation, with ROS being activated by BPH infestation, and the degree of induction was much higher in the resistant rice cultivar RHT than in the susceptible cultivar 9311 (Fig. 8, A to C). Treatment with H_2O_2 strengthened the BPH resistance of rice plants (fig. S13). In addition, *OsRbohB* was induced by BPH infestation (Fig. 7A) and positively regulated BPH resistance (fig. S9). Therefore, ROS functioned to positively regulate BPH resistance. Consistent with this conclusion, plants actively generate ROS in response to aphid infestation, a large family of sap-feeding herbivorous insects, and rapid ROS induction is often correlated with aphid resistance (*53*).

Cross-talk and coordination between and among different signaling pathways is crucial for plant development and immunity. The cross-talk between auxin and ROS is well established in root hair polar growth, which is endogenously controlled by auxin and sustained by oscillating ROS level. In *Arabidopsis*, auxin activates the crucial bHLH transcription factor ROOT HAIR DEFECTIVE 6-LIKE 4 (RSL4) through several ARFs, and RSL4 induces expression of *RbohC/J*, leading to ROS production (*54*). Furthermore, ROS are essential for the nucleo-cytoplasmic distribution of TIR1/AFB2 through facilitating their nuclear import and subsequent activation of downstream signaling (*55*). In addition, ROS function upstream of auxin signaling to mediate the response to metal stress. The promotion or repression of ROS on auxin is dynamic, with auxin signaling activated by mild stress but inhibited by severe stress (*56*, *57*). In rice, asymmetric stress induces a ROS burst and signaling to remodel root architecture to avoid localized stress, this process requires the participation of the auxin signaling pathway, but the detailed mechanism is unclear (*58*). A recent study reveals that activation of auxin in root hair formation depends on *OsRbohE* in rice (*59*). Still, the detailed mechanism remain unclear. BPH is a kind of pierce-sucking insect that could be defensed by increased auxin. In this study, we further illustrated a genetic cross-talk between auxin and ROS that mediated BPH resistance based on the OsmiR393/OsTIR1-OsIAA10-OsARF12-OsRbohB genetic pathway, with activated auxin signaling promoting ROS accumulation and thus enhancing BPH resistance. BPH infestation depresses auxin synthesis through some unknown mechanism (Fig. 1, E and F), which, in turn, induces the expression of *OsTIR1*, represses the function of OsIAA10, and thus releases *OsARF12*, which activates the downstream *OsRbohB* gene and results in resistance to BPH through increase in ROS accumulation. Meanwhile, *OsTIR1* is posttranscriptionally regulated by OsmiR393, which also participates in BPH resistance through a negative regulatory mechanism (Fig. 8Q). Comprehensively, accumulation of ROS in the BPH resistant lines of genes functioning in auxin signaling was distinctly higher, such as 393DKO (Fig. 8J), TIROE (Fig. 8K), IAA10KO (Fig. 8L), and ARF12OE (Fig. 8M), whereas ROS accumulation was lower in the BPH-susceptible lines, such as 393aOE, 393bOE (Fig. 8J), TIRKO (Fig. 8K), IAA10OE (Fig. 8L), and ARF12KO (Fig. 8M). Genetically, the high ROS concentration in the 393DKO plants was moderated by *OsARF12* knockout (Fig. 8P) and *OsRbohB* knockout (Fig. 8O), accompanied by lowered resistance to BPH, respectively (Figs. 6Q and 7L). In contrast, the low ROS concentration in the ARF12KO plants was elevated by *OsRbohB* overexpression (Fig. 8N), with the BPH susceptibility of the ARF12KO plants being promoted to a level similar to that of the WT (Fig. 7K). As a plant early immune-response marker, ROS are usually activated by BPH salivary proteins (*60*). The auxin-ROS cross-talk identified in this study might also function in rice-RBSDV interaction because ROS accumulation was distinctly reduced in the lines overexpressing OsmiR393, *OsIAA20*, or *OsIAA31* (*42*). In contrast, moderate upregulation of auxin signaling inhibits the PTI-triggered ROS burst and results in pathogen susceptibility in maize, but the underlying mechanism is uncertain (*61*). Here arises the question: Is the auxin signaling modulation of ROS through transcriptional regulation of *OsRboh* genes by OsARF a generally conserved mechanism? There are nine *OsRboh* genes in the rice genome, of which not all are

activated in the response to BPH infestation (Fig. 7A). Given the considerable number of OsARF family members in rice and that different ARFs might have varying regulatory effects on plant defense (*12*), diverse pairings of OsARF and *OsRboh* genes might have different regulatory (positive or negative) effects. Furthermore, there might be additional pathways that mediate auxin and ROS crosstalk, which deserve further research.

In summary, we revealed that, in the interaction between BPH and rice, BPH disturbs the IAA pathway and reduces the vitality of host plant for successful infestation, resulting in reduction in IAA content (Fig. 1, E and F). As a counteracting feedback mechanism, the lowered IAA content might instead activate the innate IAA signaling pathway in rice plants, with expression and function of *OsTIR1*/*OsAFB2* being promoted, of *OsARF12* being activated, whereas expression of *OsIAA10* being inhibited. The enhanced auxin signaling further promotes ROS accumulation and, thus, strengthens the defense response.

MATERIALS AND METHODS

Plant materials and BPH population

The WT rice plants used in this study were cultivars ZH11 (*O. sativa* L. subsp. *japonica* cv. Zhonghua No.11, ZH11), NIP (*O. sativa* L. subsp. *japonica*. cv. *Nip*pobare, NIP), RHT, TN1 (*O. sativa* L. subsp. *indica* cv. Taichung Native 1, TN1), 9311 (*O. sativa* L. subsp. *indica* cv. 9311, 9311), and Kasalath (*O. sativa* L. subsp. *indica* cv. Kasalath). ZH11, NIP, and Kasalath were mainly used as host of genetic transformation or natural WT of mutants. RHT was a well-known BPH-resistant cultivar, and 9311 was a well-known BPH-susceptible cultivar. TN1 was used to cultivate BPH in a climate-controlled room at 26° ± 2°C, 12-hour/12-hour light/dark cycle and 80% relative humidity. All rice plants were cultivated under field conditions at two different experimental stations in Shanghai (30°N, 121°E) and Lingshui (Hainan Province, 18°N, 110°E), China. Rice seedlings were cultured in the phytotron in CAS Center for Excellence in Molecular Plant Sciences, with 30/24° ± 1°C day/night temperature, 50 to 70% relative humidity and a light/dark period of 14 hours/10 hours was used to culture rice seedlings.

BPH resistance detection and measurements

Individual test assay was carried out at seedling stage using at least six replicates of each cultivar or line. Each seedling about 4 weeks was infested with 20 second-instar BPH nymphs. Plant status were checked daily, and, about 5 to 12 days later, when one tested line died or the contrast between the two/three tested lines is obvious, the plants were scored as susceptible (dead) or resistant (alive) and photographs taken.

For small population assay, about 40 plants of tested lines and the WT were planted in a plate in the mud for 1 month till about third-leaf stage and fed to BPH population in appropriately 8 to 10 first-instar nymphs per plant, and the plant status (alive or dead) was surveyed daily in the following days. Data were collected when one tested line died or the contrast between the two/three tested lines is obvious. Plant materials were photographed using a NIKON D7000 digital camera, and the survival rates were calculated on the basis of data from at least three repeats. Honeydew content detection was carried out as previously described (*38*).

Plasmid construction and plant transformation

For overexpression of *OsMIR393a*, fragment containing the stem-loop structure of pri-OsmiR393a was cloned into the p1301-35*S*-NOS vector using Bam HI and Kpn I double digestion. For overexpression of *OsTIR1* and *OsIAA10*, full-length cDNA of respective genes was amplified and cloned into the p1301-35*S*-Nos vector through digestion by Bam HI and Kpn I. For overexpression of *OsRbohB* gene in the ARF12KO background, full-length cDNA of *OsRbohB* was amplified and cloned into the pCAMBIA2301 vector through digestion by Bam HI and Kpn I.

For construction of knockout plants such as 393DKO-2, 393DKOk, TIR1KO, and AFB2KO, guide DNA (gDNA) was, respectively, synthesized and cloned into the pOs-sgRNA vector and then transferred to the pYLCRISPR/Cas9Pubi-H vector with hygromycin selection marker through LR reaction. Primers and gDNAs used for these genes were listed in table S1.

For RbohBKO plant construction in the 393DKO background, gDNA was synthesized and cloned into the pOs-sgRNA vector and then transferred to the pYLCRISPR/Cas9Pubi-B with vector glyphosate selection marker through LR reaction. Primers and gDNAs used for these genes were listed in table S1. Transformation of these plasmids was carried out through *Agrobacterium*-mediated genetic transformation in Biorun Biosciences Company.

RNA isolation and qRT-PCR analysis

For verification of respective transgenic plants, seedlings were used. Total RNAs were extracted using TRIzol (Life technologies, USA) and reverse transcribed using the First-Strand cDNA Synthesis Kit (Toyobo). qRT-PCR was performed with the SYBR Green Real-Time PCR Master Mix Kit (Toyobo), cDNA was synthesized from 1 μg of total RNA, and 1 μl of cDNA was used as template for real-time analysis. The rice *actin* (LOC_Os03g50885) and *ubiquitin* (LOC_Os01g22490) genes were used as reference genes to normalize expression levels. Data from three biological repeats were collected, and the mean value with standard error was plotted. For gene expression assay responsive to BPH, around 2-week-old rice seedlings were individually infested with 12 second-instar BPH nymphs that had been starved for 2 hours; leaf sheaths and leaves were collected after 0, 2, 4, 8, 12, 24, and 48 hours for RNA extraction followed by reverse transcription and qRT-PCR. All the primer sequences used in qRT-PCR and other analysis in this study were listed in table S1.

miRNA Northern blot analysis and qRT-PCR analysis

miRNA Northern blot was carried out as previously described (*36*). Specifically, leaves of the rice seedlings were used for RNA extraction, and the OsmiR393 probe was synthesized with 5′-end biotin. The blots were incubated at 42°C for 30 min in the Hybridization Buffer (Ambion). In addition, 50 to 80 pM probes were added in the hybridization buffer to incubate for one night. For RNA loading, 5*S* ribosomal RNA was used as control.

qRT-PCR analysis of miRNA was carried out as described (*36*, *62*) using the miRNA First-Strand cDNA Synthesis Kit (Vazyme Biotech, China) and miRNA Universal SYBR qPCR Master Mix (Vazyme Biotech, China). The $2^{-\Delta\Delta CT}$ method was used to quantify relative gene expression levels. Mean of internal reference gene *U6* was used for normalization.

LCI assay

The full-length cDNA of the *OsTIR1* and *OsIAA10* genes and that of *OsIAA10* and *OsARF12* genes were, respectively, cloned into the Kpn I and Sal I sites of pCAMBIA1300-CLuc and pCAMBIA1300-NLuc using homologous recombination. All the constructs for test

were transformed into *Agrobacterium tumefaciens* GV3101 (pSoup-P19). *Agrobacterium* cells were resuspended in infection solution (10 mM MES, 10 mM $MgCl_2$, and 200 μM acetosyringone) at optical density at 600 nm (OD_{600}) of 1.0. The prepared suspensions were infiltrated into *N. benthamiana* leaves. At 3 days post-infiltration, the LUC signal was detected using a charge-coupled device (CCD) camera and a luciferin solution (150 mg/ml).

Co-IP assay

The full-length cDNA of *OsARF12* was fused with the FLAG tag, while the full-length cDNA of *OsIAA10* was fused with the green fluorescent protein (GFP) tag. The recombinant and control vectors were transformed into *Agrobacterium* GV3101, which were then resuspended in infection solution at OD_{600} of 1.0. The prepared suspensions were infiltrated into *N. benthamiana* leaves, which were harvested after 3 days and frozen in liquid nitrogen. Soluble proteins were extracted with NB1 buffer [50 mM tris-MES (pH 8.0), 500 mM sucrose, 1 mM $MgCl_2$, 10 mM EDTA, 5 mM dithiothreitol, 1 mM phenylmethylsulfonyl fluoride, and cocktail]. Immunoprecipitation was performed with anti-FLAG-affinity beads (Sigma-Aldrich). Lysates were incubated with the prewashed beads for 3 hours. Then, the beads were washed six times and solubilized in an appropriate volume of extraction buffer with 1× SDS loading buffer. The fusion proteins were detected by immunoblotting using monoclonal anti-FLAG M2 antibody (Sigma-Aldrich) and monoclonal antibody anti-GFP (Huabio).

Bimolecular fluorescence complementation

The cDNA of *OsIAA10*, *OsTIR1*, and *OsARF12* were, respectively, cloned into the Kpn I and Sal I sites of pCAMBIA1300-35*S*-cYFP and pCAMBIA1300-35*S*-nYFP using homologous recombination. Experiment design was carried out according to previously report (*63*). The recombinant and control vectors were transformed into *Agrobacterium* GV3101, respectively. *Agrobacterium* cells were resuspended in infection solution at OD_{600} of 1.0. The prepared suspensions were infiltrated into *N. benthamiana* leaves. After culture for 3 days, the signals of yellow fluorescent protein and mCherry were detected using confocal microscopy (LSM 880; Zeiss).

Y2H assay

The cDNAs of *OsIAA10* and *OsTIR1* were, respectively, cloned into the Bam HI site of pGBKT7 using homologous recombination to get BD-IAA10 and BD-TIR1 plasmid. Similarly, the cDNAs of *OsIAA10* and *OsARF12* were, respectively, cloned into the Bam HI site of pGADT7 to get AD-IAA10 and AD-ARF12 plasmids. The plasmids were transformed into AH109 strain after pairing using a lithium acetate transformation protocol (Yeast Protocols Handbook PT3024-1; Clontech) and cultured at 30°C on SD/-Leu-Trp for 2 days. The transformed yeast colonies were suspended in sterilized water (OD_{600} of 1.0) and grown on SD/-Leu-Trp and SD/-Leu-Trp-Ade-His media in a 10^{-1}, 10^{-2}, and 10^{-3} gradient. Specially, in the selection of the OsTIR1-interacting OsIAAs, 10 μM IAA was added to the SD/-Leu-Trp-His media. Photographs were taken after culture at 30°C for 3 days.

Dual-LUC assay

For transcriptional activity assays, the GAL4/UAS system was used. The VP16 transcriptional activation domain and full-length coding sequences (CDSs) of the OsARF12 fused with the GAL4 DBD were inserted into the pCAMBIA1300-Nos vector as effectors. The GAL4 DBD was inserted into the pCAMBIA1300-Nos vector as control. A sequence comprising six repeats of the GAL4-binding upstream active sequence (6xUAS), TATA-Box, and 35*S* promoter was synthesized and cloned into the pGreenII0800-LUC to generate the 35*S*-UAS-TATA-LUC reporter plasmid.

For the binding activity assays, the 2000–base pair (bp) genomic fragment upstream of the *OsRbohB* start codon 'ATG' was cloned into the pGreenII0800-LUC vector as the reporter. The full-length CDSs of the *OsARF12* were cloned into the pHB vector as effector. The pHB empty vector was used as negative control.

In the GAL4/UAS system and the dual-LUC assay, all the recombinant constructs were transformed into *A. tumefaciens* strain GV3101 (pSoup-P19) and then transiently expressed in *N. benthamiana*. At 48 to 72 hours post-infiltration, the leaves were examined using a CCD camera and a luciferin solution (150 μg/ml). Alternatively, luciferase activity was quantified using a luminometer according to the manufacturer's instructions (Promega).

Electrophoretic mobility shift assay

For protein expression and purification, the N-terminal sequence encoding the 1 to 247 amino acids of *OsARF12* was cloned into the pCold-TF vector. The resulting recombinant plasmid was transformed into *Escherichia coli* BL21 (DE3) cells to produce the His-tagged fusion protein. The Cyanine 5 (Cy5)-labeled probe was amplified by two rounds of PCR. The DNA probes and proteins were co-incubated in the reaction buffer, purified, and incubated with the Cy5-labeled probe at 37°C for 20 min in EMSA buffer [25 mM Hepes (pH 7.5), 40 mM potassium chloride, 3 mM dithiothreitol, 10% glycerol, 0.1 mM EDTA, bovine serum albumin (0.5 mg/ml), and poly-glutamate (0.5 mg/ml)]. After incubation, the reaction mixture was electrophoresed on a 6% native polyacrylamide gel, and the labeled DNA was then detected using a Starion FLA-9000 instrument.

In vitro ChIP-qPCR

For ChIP-qPCR, nuclei of 2-week-old ARF12OE plants were extracted, purified, and sonicated to obtain DNA fragments of 300 to 500 bp using a Bioruptor UCD-200. The fragments were precleared with ChIP protein A/G beads (Merck) for 1 hour before incubation for another 1 hour in new protein A/G beads with antibody. The anti-ARF12 antibody was used for test, while the anti-IgG antibody was used as control. The beads were then washed twice with low-salt and high-salt buffer, respectively. The washed magnetic beads were directly reverse cross-linked, and the DNA fragments were purified and used as template for quantitative PCR. Primers used for ChIP assays are listed in table S1.

DAB staining and measurement of H_2O_2

Accumulation of H_2O_2 was detected by DAB staining as described previously (*64*). Leaves were cut into small pieces (1 cm in length) and vacuum infiltrated in DAB solution [DAB (1 mg/ml) and 10 mM MES (pH 3.8) with 0.2% (v/v) Tween 20] for 5 min. After further incubation at 25°C for 8 hours, samples were cleared by boiling in 96% ethanol for 10 min. The cleared samples were mounted in 50% glycerol for imaging (Leica M205FA).

Quantification of H_2O_2 was performed using a Hydrogen Peroxide Content Assay Kit (Sangon Biotech) following the manufacturer's instruction. The samples were frozen in liquid nitrogen and ground into fine powders. Each sample (100 mg) was fully suspended in 1 ml of acetone. The extracts were centrifuged at 8000*g*

for 10 min at 4°C, and the supernatant was used for quantification. The concentration of H_2O_2 was shown as micromoles per gram of fresh weight.

ROS measurement

For measurement of ROS bursts in rice cells after chitin treatment, the luminol chemiluminescence assay was conducted (*65*). Leaf sheaths from 2-week-old rice seedlings cultivated in nutrient solution were cut into ~3-mm strips and preincubated overnight in sterile distilled water to recover from wounding stress. The materials were then treated with 1×10^{-6} M chitin [octa-*N*-acetylchitooctaose $(GlcNAc)_8$] or water as a control in reaction buffer containing 20 μM luminol (Wako) and horseradish peroxidase (10 μg ml^{-1}; Sigma-Aldrich). Luminescence was monitored immediately after the treatment and continuously measured at 2 min intervals for 40 min with Varioskan Flash multireader (Thermo Fisher Scientific).

Quantification of IAA

The leaf sheaths of rice seedlings were collected at different time points after BPH infestation, and ethyl acetate was added for extraction after grinding in liquid nitrogen. Nitrogen blowing is followed by reconstitution with methanol. IAA level was analyzed by high-performance liquid chromatography–mass spectrometry using labeled internal standard.

Auxin (NAA) treatment assays

Seedlings were grown in 7 cm–by–7 cm–by–8.5 cm pots in 5 × 5 pattern. Around 4-week-old seedlings were grouped for different concentration of NAA treatment, first immersed the seedling in corresponding NAA solution and then kept breeding the seedlings with the same concentration of NAA solution, and fed to BPH population 2 hours later, with 8 to 10 first-instar nymphs for each seedling. The seedlings were gently plucked to let the BPH scatter uniformly. In the following days, the status of the plants (alive or dead) were surveyed daily.

Primer sequences

All the oligo sequences used in this study are listed in table S1.

Statistical analysis

All data values for the statistical analysis were presented in table S2, corresponding to each figures.

Supplementary Materials

The PDF file includes:
Figs. S1 to S13
Legends for tables S1 and S2

Other Supplementary Material for this manuscript includes the following:
Tables S1 and S2

REFERENCES AND NOTES

1. S. Min, S. W. Lee, B.-R. Choi, S. H. Lee, D. H. Kwon, Insecticide resistance monitoring and correlation analysis to select appropriate insecticides against *Nilaparvata lugens* (Stål), a migratory pest in Korea. *J. Asia Pac. Entomol.* **17**, 711–716 (2014).
2. C. M. Pieterse, D. Van der Does, C. Zamioudis, A. Leon-Reyes, S. C. Van Wees, Hormonal modulation of plant immunity. *Annu. Rev. Cell Dev. Biol.* **28**, 489–521 (2012).
3. L. I. Calderon-Villalobos, X. Tan, N. Zheng, M. Estelle, Auxin perception—Structural insights. *Cold Spring Harb. Perspect. Biol.* **2**, a005546 (2010).
4. C. Cance, R. Martin-Arevalillo, K. Boubekeur, R. Dumas, Auxin response factors are keys to the many auxin doors. *New Phytol.* **235**, 402–419 (2022).
5. D. Wang, K. Pei, Y. Fu, Z. Sun, S. Li, H. Liu, K. Tang, B. Han, Y. Tao, Genome-wide analysis of the auxin response factors (ARF) gene family in rice (*Oryza sativa*). *Gene* **394**, 13–24 (2007).
6. J. W. Chandler, Auxin response factors. *Plant Cell Environ.* **39**, 1014–1028 (2016).
7. X. Song, Y. Xiong, X. Kong, G. Huang, Roles of auxin response factors in rice development and stress responses. *Plant Cell Environ.* **46**, 1075–1086 (2023).
8. B. N. Kunkel, J. M. B. Johnson, Auxin plays multiple roles during plant-pathogen interactions. *Cold Spring Harb. Perspect. Biol.* **13**, a040022 (2021).
9. B. N. Kidd, N. Y. Kadoo, B. Dombrecht, M. Tekeoglu, D. M. Gardiner, L. F. Thatcher, E. A. Aitken, P. M. Schenk, J. M. Manners, K. Kazan, Auxin signaling and transport promote susceptibility to the root-infecting fungal pathogen *Fusarium oxysporum* in *Arabidopsis*. *Mol. Plant Microbe Interact.* **24**, 733–748 (2011).
10. L. Jin, Q. Qin, Y. Wang, Y. Pu, L. Liu, X. Wen, S. Ji, J. Wu, C. Wei, B. Ding, Y. Li, Rice dwarf virus P2 protein hijacks auxin signaling by directly targeting the rice OsIAA10 protein, enhancing viral infection and disease development. *PLOS Pathog.* **12**, e1005847 (2016).
11. H. Zhang, L. Li, Y. He, Q. Qin, C. Chen, Z. Wei, X. Tan, K. Xie, R. Zhang, G. Hong, J. Li, J. Li, C. Yan, F. Yan, Y. Li, J. Chen, Z. Sun, Distinct modes of manipulation of rice auxin response factor OsARF17 by different plant RNA viruses for infection. *Proc. Natl. Acad. Sci. U.S.A.* **117**, 9112–9121 (2020).
12. Q. Qin, G. Li, L. Jin, Y. Huang, Y. Wang, C. Wei, Z. Xu, Z. Yang, H. Wang, Y. Li, Auxin response factors (ARFs) differentially regulate rice antiviral immune response against rice dwarf virus. *PLOS Pathog.* **16**, e1009118 (2020).
13. J. Qi, J. Wang, Z. Gong, J. M. Zhou, Apoplastic ROS signaling in plant immunity. *Curr. Opin. Plant Biol.* **38**, 92–100 (2017).
14. M. Gao, Y. He, X. Yin, X. Zhong, B. Yan, Y. Wu, J. Chen, X. Li, K. Zhai, Y. Huang, X. Gong, H. Chang, S. Xie, J. Liu, J. Yue, J. Xu, G. Zhang, Y. Deng, E. Wang, D. Tharreau, G. L. Wang, W. Yang, Z. He, Ca^{2+} sensor-mediated ROS scavenging suppresses rice immunity and is exploited by a fungal effector. *Cell* **184**, 5391–5404.e17 (2021).
15. G. Miller, K. Schlauch, R. Tam, D. Cortes, M. A. Torres, V. Shulaev, J. L. Dangl, R. Mittler, The plant NADPH oxidase RBOHD mediates rapid systemic signaling in response to diverse stimuli. *Sci. Signal.* **2**, ra45 (2009).
16. C. Zipfel, G. E. Oldroyd, Plant signalling in symbiosis and immunity. *Nature* **543**, 328–336 (2017).
17. J. D. Jones, J. L. Dangl, The plant immune system. *Nature* **444**, 323–329 (2006).
18. C. Waszczak, M. Carmody, J. Kangasjarvi, Reactive oxygen species in plant signaling. *Annu. Rev. Plant Biol.* **69**, 209–236 (2018).
19. B. C. Tripathy, R. Oelmuller, Reactive oxygen species generation and signaling in plants. *Plant Signal. Behav.* **7**, 1621–1633 (2012).
20. L. Cao, S. Karapetyan, H. Yoo, T. Chen, M. Mwimba, X. Zhang, X. Dong, H_2O_2 sulfenylates CHE, linking local infection to the establishment of systemic acquired resistance. *Science* **385**, 1211–1217 (2024).
21. M. A. Torres, J. L. Dangl, J. D. Jones, Arabidopsis gp91phox homologues AtrbohD and AtrbohF are required for accumulation of reactive oxygen intermediates in the plant defense response. *Proc. Natl. Acad. Sci. U.S.A.* **99**, 517–522 (2002).
22. H. Yoshioka, S. Asai, M. Yoshioka, M. Kobayashi, Molecular mechanisms of generation for nitric oxide and reactive oxygen species, and role of the radical burst in plant immunity. *Mol. Cells* **28**, 321–330 (2009).
23. L. Denness, J. F. McKenna, C. Segonzac, A. Wormit, P. Madhou, M. Bennett, J. Mansfield, C. Zipfel, T. Hamann, Cell wall damage-induced lignin biosynthesis is regulated by a reactive oxygen species- and jasmonic acid-dependent process in Arabidopsis. *Plant Physiol.* **156**, 1364–1374 (2011).
24. C. Bowler, R. Fluhr, The role of calcium and activated oxygens as signals for controlling cross-tolerance. *Trends Plant Sci.* **5**, 241–246 (2000).
25. S. M. Coelho, A. R. Taylor, K. P. Ryan, I. Sousa-Pinto, M. T. Brown, C. Brownlee, Spatiotemporal patterning of reactive oxygen production and Ca^{2+} wave propagation in fucus rhizoid cells. *Plant Cell* **14**, 2369–2381 (2002).
26. A. Baxter-Burrell, Z. Yang, P. S. Springer, J. Bailey-Serres, RopGAP4-dependent Rop GTPase rheostat control of Arabidopsis oxygen deprivation tolerance. *Science* **296**, 2026–2028 (2002).
27. S. K. Jalmi, A. K. Sinha, ROS mediated MAPK signaling in abiotic and biotic stress- striking similarities and differences. *Front. Plant Sci.* **6**, 769 (2015).
28. V. B. Tognetti, A. Bielach, M. Hrtyan, Redox regulation at the site of primary growth: Auxin, cytokinin and ROS crosstalk. *Plant Cell Environ.* **40**, 2586–2605 (2017).
29. J. H. Joo, Y. S. Bae, J. S. Lee, Role of auxin-induced reactive oxygen species in root gravitropism. *Plant Physiol.* **126**, 1055–1060 (2001).
30. M. S. Biswas, H. Fukaki, I. C. Mori, K. Nakahara, J. Mano, Reactive oxygen species and reactive carbonyl species constitute a feed-forward loop in auxin signaling for lateral root formation. *Plant J.* **100**, 536–548 (2019).
31. X. Qi, Q. Li, X. Ma, C. Qian, H. Wang, N. Ren, C. Shen, S. Huang, X. Xu, Q. Xu, X. Chen, Waterlogging-induced adventitious root formation in cucumber is regulated by ethylene and auxin through reactive oxygen species signalling. *Plant Cell Environ.* **42**, 1458–1470 (2019).

32. X. Song, Y. Li, X. Cao, Y. Qi, MicroRNAs and their regulatory roles in plant-environment interactions. *Annu. Rev. Plant Biol.* **70**, 489–525 (2019).
33. Z. Dai, J. Tan, C. Zhou, X. Yang, F. Yang, S. Zhang, S. Sun, X. Miao, Z. Shi, The OsmiR396-OsGRF8-OsF3H-flavonoid pathway mediates resistance to the brown planthopper in rice (*Oryza sativa*). *Plant Biotechnol. J.* **17**, 1657–1669 (2019).
34. Y. Ge, J. Han, G. Zhou, Y. Xu, Y. Ding, M. Shi, C. Guo, G. Wu, Silencing of miR156 confers enhanced resistance to brown planthopper in rice. *Planta* **248**, 813–826 (2018).
35. Y. Shen, G. Yang, X. Miao, Z. Shi, OsmiR159 modulate BPH resistance through regulating G-protein gamma subunit GS3 gene in rice. *Rice* **16**, 30 (2023).
36. B. Sun, Y. Shen, L. Zhu, X. Yang, X. Liu, D. Li, M. Zhu, X. Miao, Z. Shi, OsmiR319-OsPCF5 modulate resistance to brown planthopper in rice through association with MYB proteins. *BMC Biol.* **22**, 68 (2024).
37. K. Xia, R. Wang, X. Ou, Z. Fang, C. Tian, J. Duan, Y. Wang, M. Zhang, OsTIR1 and OsAFB2 downregulation via OsmiR393 overexpression leads to more tillers, early flowering and less tolerance to salt and drought in rice. *PLOS ONE* **7**, e30039 (2012).
38. B. Du, W. Zhang, B. Liu, J. Hu, Z. Wei, Z. Shi, R. He, L. Zhu, R. Chen, B. Han, G. He, Identification and characterization of Bph14, a gene conferring resistance to brown planthopper in rice. *Proc. Natl. Acad. Sci. U.S.A.* **106**, 22163–22168 (2009).
39. M. Jain, N. Kaur, R. Garg, J. K. Thakur, A. K. Tyagi, J. P. Khurana, Structure and expression analysis of early auxin-responsive *Aux/IAA* gene family in rice (*Oryza sativa*). *Funct. Integr. Genomics* **6**, 47–59 (2006).
40. Z. X. Zhao, Q. Feng, X. L. Cao, Y. Zhu, H. Wang, V. Chandran, J. Fan, J. Q. Zhao, M. Pu, Y. Li, W. M. Wang, *Osa-miR167d* facilitates infection of *Magnaporthe oryzae* in rice. *J. Integr. Plant Biol.* **62**, 702–715 (2020).
41. Y. Shi, Y. L. Chang, H. T. Wu, A. Shalmani, W. T. Liu, W. Q. Li, J. W. Xu, K. M. Chen, OsRbohB-mediated ROS production plays a crucial role in drought stress tolerance of rice. *Plant Cell Rep.* **39**, 1767–1784 (2020).
42. H. Zhang, X. Tan, L. Li, Y. He, G. Hong, J. Li, L. Lin, Y. Cheng, F. Yan, J. Chen, Z. Sun, Suppression of auxin signalling promotes rice susceptibility to Rice black streaked dwarf virus infection. *Mol. Plant Pathol.* **20**, 1093–1104 (2019).
43. J. Chen, Y. Zhao, X. Luo, H. Hong, T. Yang, S. Huang, C. Wang, H. Chen, X. Qian, M. Feng, Z. Chen, Y. Dong, Z. Ma, J. Li, M. Zhu, S. Y. He, S. P. Dinesh-Kumar, X. Tao, NLR surveillance of pathogen interference with hormone receptors induces immunity. *Nature* **613**, 145–152 (2023).
44. K. Kazan, R. Lyons, Intervention of phytohormone pathways by pathogen effectors. *Plant Cell* **26**, 2285–2309 (2014).
45. M. Naseem, M. Srivastava, M. Tehseen, N. Ahmed, Auxin crosstalk to plant immune networks: A plant-pathogen interaction perspective. *Curr. Protein Pept. Sci.* **16**, 389–394 (2015).
46. L. Navarro, P. Dunoyer, F. Jay, B. Arnold, N. Dharmasiri, M. Estelle, O. Voinnet, J. D. Jones, A plant miRNA contributes to antibacterial resistance by repressing auxin signaling. *Science* **312**, 436–439 (2006).
47. G. Shi, S. Wang, P. Wang, J. Zhan, Y. Tang, G. Zhao, F. Li, X. Ge, J. Wu, Cotton miR393-TIR1 module regulates plant defense against verticillium dahliae via auxin perception and signaling. *Front. Plant Sci.* **13**, 888703 (2022).
48. S. Werghi, F. A. Herrero, H. Fakhfakh, F. Gorsane, Auxin drives tomato spotted wilt virus (TSWV) resistance through epigenetic regulation of auxin response factor ARF8 expression in tomato. *Gene* **804**, 145905 (2021).
49. D. Wang, M. Yuan, Y. Zhuang, X. F. Xin, G. Qi, DGK5-mediated phosphatidic acid homeostasis interplays with reactive oxygen species in plant immune signaling. *J. Integr. Plant Biol.* **66**, 1263–1265 (2024).
50. M. F. Ali, G. K. Muday, Reactive oxygen species are signaling molecules that modulate plant reproduction. *Plant Cell Environ.* **47**, 1592–1605 (2024).
51. L. Li, M. Li, L. Yu, Z. Zhou, X. Liang, Z. Liu, G. Cai, L. Gao, X. Zhang, Y. Wang, S. Chen, J. M. Zhou, The FLS2-associated kinase BIK1 directly phosphorylates the NADPH oxidase RbohD to control plant immunity. *Cell Host Microbe* **15**, 329–338 (2014).
52. G. B. Li, J. X. He, J. L. Wu, H. Wang, X. Zhang, J. Liu, X. H. Hu, Y. Zhu, S. Shen, Y. F. Bai, Z. L. Yao, X. X. Liu, J. H. Zhao, D. Q. Li, Y. Li, F. Huang, Y. Y. Huang, Z. X. Zhao, J. W. Zhang, S. X. Zhou, Y. P. Ji, M. Pu, P. Qin, S. Li, X. Chen, J. Wang, M. He, W. Li, X. J. Wu, Z. J. Xu, W. M. Wang, J. Fan, Overproduction of OsRACK1A, an effector-targeted scaffold protein promoting OsRBOHB-mediated ROS production, confers rice floral resistance to false smut disease without yield penalty. *Mol. Plant* **15**, 1790–1806 (2022).
53. F. L. Goggin, H. D. Fischer, Reactive oxygen species in plant interactions with Aphids. *Front. Plant Sci.* **12**, 811105 (2021).
54. S. Mangano, S. P. Denita-Juarez, H. S. Choi, E. Marzol, Y. Hwang, P. Ranocha, S. M. Velasquez, C. Borassi, M. L. Barberini, A. A. Aptekmann, J. P. Muschietti, A. D. Nadra, C. Dunand, H. T. Cho, J. M. Estevez, Molecular link between auxin and ROS-mediated polar growth. *Proc. Natl. Acad. Sci. U.S.A.* **114**, 5289–5294 (2017).
55. B. Lu, S. Wang, H. Feng, J. Wang, K. Zhang, Y. Li, P. Wu, M. Zhang, Y. Xia, C. Peng, C. Li, FERONIA-mediated TIR1/AFB2 oxidation stimulates auxin signaling in Arabidopsis. *Mol. Plant* **17**, 772–787 (2024).
56. N. Parveen, N. Kandhol, S. Sharma, V. P. Singh, D. K. Chauhan, J. Ludwig-Muller, F. J. Corpas, D. K. Tripathi, Auxin crosstalk with reactive oxygen and nitrogen species in plant development and abiotic stress. *Plant Cell Physiol.* **63**, 1814–1825 (2023).
57. L. Demecsova, L. Tamas, Reactive oxygen species, auxin and nitric oxide in metal-stressed roots: Toxicity or defence. *Biometals* **32**, 717–744 (2019).
58. H. Q. Wang, X. Y. Zhao, W. Xuan, P. Wang, F. J. Zhao, Rice roots avoid asymmetric heavy metal and salinity stress via an RBOH-ROS-auxin signaling cascade. *Mol. Plant* **16**, 1678–1694 (2023).
59. X. Y. Zhao, H. Q. Wang, W. Shi, W. W. Zhang, F. J. Zhao, The respiratory burst oxidase homologue OsRBOHE is crucial for root hair formation, drought resistance and tillering in rice. *Plant Cell Environ.* **48**, 65–80 (2024).
60. J. Fu, Y. Shi, L. Wang, H. Zhang, J. Li, J. Fang, R. Ji, Planthopper-secreted salivary disulfide isomerase activates immune responses in plants. *Front. Plant Sci.* **11**, 622513 (2020).
61. F. Navarrete, M. Gallei, A. E. Kornienko, I. Saado, M. Khan, K. S. Chia, M. A. Darino, J. Bindics, A. Djamei, TOPLESS promotes plant immunity by repressing auxin signaling and is targeted by the fungal effector Naked1. *Plant Commun.* **3**, 100269 (2022).
62. C. Chen, D. A. Ridzon, A. J. Broomer, Z. Zhou, D. H. Lee, J. T. Nguyen, M. Barbisin, N. L. Xu, V. R. Mahuvakar, M. R. Andersen, K. Q. Lao, K. J. Livak, K. J. Guegler, Real-time quantification of microRNAs by stem-loop RT-PCR. *Nucleic Acids Res.* **33**, e179 (2005).
63. J. Kudla, R. Bock, Lighting the way to protein-protein interactions: Recommendations on best practices for bimolecular fluorescence complementation analyses. *Plant Cell* **28**, 1002–1008 (2016).
64. X. Yin, B. Zou, X. Hong, M. Gao, W. Yang, X. Zhong, Y. He, P. Kuai, Y. Lou, J. Huang, J. Hua, Z. He, Rice copine genes OsBON1 and OsBON3 function as suppressors of broad-spectrum disease resistance. *Plant Biotechnol. J.* **16**, 1476–1487 (2018).
65. K. Zhai, D. Liang, H. Li, F. Jiao, B. Yan, J. Liu, Z. Lei, L. Huang, X. Gong, X. Wang, J. Miao, Y. Wang, J. Y. Liu, L. Zhang, E. Wang, Y. Deng, C. K. Wen, H. Guo, B. Han, Z. He, NLRs guard metabolism to coordinate pattern- and effector-triggered immunity. *Nature* **601**, 245–251 (2022).

Acknowledgments: We are grateful for C. Miao from Hainan Agricultural University for providing 393DKO-1 seeds; H. Bian from Zhejiang University for providing 393bOE seeds; Y. Li from Peking University for providing OsIAA10KO, ARF12OE, and ARF12KO seeds; K. Chen from Lanzhou University for providing *osrbohB* seeds; and T. Peng from Henan Agricultural University for providing OsARF12OE seeds in NIP genetic background. We thank R. McKenzie from Liwen Bianji (Edanz) (www.liwenbianji.cn) for editing the English text of a draft of this manuscript. **Funding:** This work was supported by the Agriculture Research System of Shanghai, China (202403, L.C.); National Natural Science Foundation of China (32072029, Z.S.); and open project of National Key Laboratory of Crop Genetic Improvement (ZK202501, Z.S.).
Author contributions: Conceptualization: X.M., L.C., and Z.S. Methodology: L.Z., H.L., and Z.T. Investigation: H.L., F.M., and S.W. Visualization: L.Z. and Z.S. Supervision: X.M., L.C., and Z.S. Writing—original draft: L.Z. and Z.S. Writing—review and editing: L.Z., X.M., L.C., and Z.S.
Competing interests: The authors declare that they have no competing interests. **Data and materials availability:** All data needed to evaluate the conclusions in the paper are present in the paper and/or the Supplementary Materials.

Submitted 16 November 2024
Accepted 10 April 2025
Published 16 May 2025
10.1126/sciadv.adu6722